NEOPLASIA
www.neoplasia.com

Volume 13 Number 10 October 2011 pp. 947–960 947

B Cells Are Critical to T-cell–Mediated Antitumor Immunity Induced by a Combined Immune-Stimulatory/ Conditionally Cytotoxic Therapy for Glioblastoma[1,2]

Marianela Candolfi[*,†,‡,§,3], James F. Curtin[*,†,‡,§], Kader Yagiz[*,†,‡,§], Hikmat Assi[*,†,‡,§], Mia K. Wibowo[*,†,‡,§], Gabrielle E. Alzadeh[*,†,‡,§], David Foulad[*,†,‡,§], AKM G. Muhammad[*,†,‡,§], Sofia Salehi[†,‡,¶], Naomi Keech[†,‡,¶], Mariana Puntel[*,†,‡,§], Chunyan Liu[*,†,‡,§], Nicholas R. Sanderson[*,†,‡,§], Kurt M. Kroeger[*,†,‡,§], Robert Dunn[#], Gislaine Martins[†,‡,¶], Pedro R. Lowenstein[*,†,‡,§,,4] and Maria G. Castro[*,†,‡,§,**,4]**

*Gene Therapeutics Research Institute, Cedars-Sinai Medical Center, Los Angeles, CA, USA; [†]Department of Biomedical Sciences, Cedars-Sinai Medical Center, Los Angeles, CA, USA; [‡]Department of Medicine, David Geffen School of Medicine, UCLA, Los Angeles, CA, USA; [§]Department of Molecular and Medical Pharmacology, David Geffen School of Medicine, UCLA, Los Angeles, CA, USA; [¶]Inflammatory Bowel and Immunobiology Research Institute, Cedars-Sinai Medical Center, Los Angeles, CA, USA; [#]Biogen Idec, Immunology/Allergy, San Diego, CA, USA; **The Brain Research Institute, and Jonsson Comprehensive Cancer Center, David Geffen School of Medicine, UCLA, Los Angeles, CA, USA

Abstract

We have demonstrated that modifying the tumor microenvironment through intratumoral administration of adenoviral vectors (Ad) encoding the conditional cytotoxic molecule, i.e., HSV1-TK and the immune-stimulatory cytokine, i.e., *fms*-like tyrosine kinase 3 ligand (Flt3L) leads to T-cell–dependent tumor regression in rodent models of glioblastoma. We investigated the role of B cells during immune-mediated glioblastoma multiforme regression. Although treatment with Ad-TK+Ad-Flt3L induced tumor regression in 60% of wild-type (WT) mice, it completely failed in B-cell–deficient Igh6$^{-/-}$ mice. Tumor-specific T-cell precursors were detected in Ad-TK+Ad-Flt3L–treated WT mice but not in Igh6$^{-/-}$ mice. The treatment also failed in WT mice depleted of total B cells or marginal zone B cells. Because we could not detect circulating antibodies against tumor cells and the treatment was equally efficient in

Abbreviations: GBM, glioblastoma multiforme; TK, thymidine kinase; Flt3L, *fms*-like tyrosine kinase 3; WT, wild-type; APC, antigen-presenting cell; Ad, adenoviral vector; MZB, marginal zone B cell; LN, lymph node; MLR, mixed leukocyte reaction; GFP, green fluorescent protein; DC, dendritic cell

Address all correspondence to: Dr. Maria G. Castro, Department of Neurosurgery, Department of Cell and Developmental Biology, University of Michigan School of Medicine, 4570 MSRB II, 1150 W Medical Center Dr, Ann Arbor, MI 48109-0650. E-mail: mariacas@umich.edu

[1]This work was supported by National Institutes of Health/National Institute of Neurological Disorders & Stroke (NIH/NINDS) grants 1R21-NS054143, 1UO1 NS052465, and 1RO1-NS057711 to M.G.C.; NIH/NINDS grants 1RO1-NS 054193 and 1RO1-NS061107 to P.R.L.; and NIH grant 1R21-AI83948-01 IBIRI-CSMC to G.M. This work was also supported by the Bram and Elaine Goldsmith and the Medallions Group Endowed Chairs in Gene Therapeutics to P.R.L. and M.G.C., respectively, and by the Drown Foundation, the Linda Tallen & David Paul Kane Foundation Annual Fellowship, and the Board of Governors at Cedars-Sinai Medical Center. M.C. was supported by an NIH/NINDS 1F32 NS058156 fellowship.

[2]This article refers to supplementary materials, which are designated by Table W1 and Figures W1 to W4 and are available online at www.neoplasia.com.

[3]Present address: Instituto de Investigaciones Biomédicas (INBIOMED), Facultad de Medicina, Universidad de Buenos Aires, Buenos Aires, Argentina.
[4]Present address: Department of Neurosurgery, Department of Cell and Developmental Biology, University of Michigan School of Medicine, Ann Arbor, MI 48109.

Received 22 July 2011; Revised 19 August 2011; Accepted 23 August 2011

DOI 10.1593/neo.11024

WT mice and in mice with B-cell–specific deletion of *Prdm 1* (encoding Blimp-1), in which B cells are present but unable to fully differentiate into antibody-secreting plasma cells, tumor regression in this model is not dependent on B cells' production of tumor antigen–specific immunoglobulins. Instead, B cells seem to play a role as antigen-presenting cells (APCs). Treatment with Ad-TK+Ad-Flt3L led to an increase in the number of B cells in the cervical lymph nodes, which stimulated the proliferation of syngeneic T cells and induced clonal expansion of antitumor T cells. Our data show that B cells act as APCs, playing a critical role in clonal expansion of tumor antigen–specific T cells and brain tumor regression.

Neoplasia (2011) 13, 947–960

Introduction

Glioblastoma multiforme (GBM) is a malignant brain cancer, accounting for approximately 50% of newly diagnosed primary brain tumors in the United States. GBM has a dismal prognosis owing to the local infiltrative tumor growth that makes complete surgical resection virtually impossible, the intrinsic radiotherapy and chemotherapy resistance of glioma cells, and their high rate of mutation. Novel therapeutic strategies such as vaccination/immunotherapies have been developed to target GBM cells disseminated throughout the brain [1]. We developed an anti-GBM immunotherapeutic approach based on engineering the tumor microenvironment, which uses a combined conditional cytotoxic/immune–stimulatory gene therapeutic modality. It consists of an adenoviral vector (Ad) encoding herpes simplex virus type I–thymidine kinase (Ad-TK), which, in the presence of ganciclovir, kills proliferating cells, and a second Ad encoding *fms*-like tyrosine kinase 3 ligand (Ad-Flt3L), which recruits antigen-presenting cells (APCs) to the brain tumor microenvironment [2]. We have shown that this combination therapy induces an antitumor immune response and immunologic memory [2–4]. While the role of cytotoxic T cells in the clearance of peripheral and brain tumors has been well documented, the role of B cells in antitumor immunity has remained debatable. This is due to several reasons: 1) increased numbers of tumor-infiltrating B lymphocytes can correlate with poor prognosis of patients harboring metastatic carcinomas [5] or with improved survival of breast carcinoma patients [6,7]; 2) resting B cells have been implicated in promoting carcinogenesis by exacerbating inflammation [8]; 3) although B cells are relatively abundant, the frequency of B cells bearing a BcR specific for a particular antigen is very low (between 10^{-4} and 10^{-5}), potentially limiting the effectiveness of B cells as APCs during initial priming of immune responses [9]; and 4) studies in B-cell knockout mice revealed that B cells actually suppress the development of immune responses *in vivo* against lymphoma, colon cancer, and melanoma (but not sarcomas) [10,11] and depletion of B lymphocytes enhances melanoma vaccination efficacy [12], whereas in separate studies, B lymphocytes were implicated in promoting fibrosarcoma tumor regression [13].

Bone marrow–derived B cells develop into either follicular B cells or marginal zone B cells (MZB) in the spleen. Follicular B cells ($B220^{+}/CD23^{high}/CD21^{low}$), which account for most peripheral mature B cells, are found in the circulation, the germinal center of peripheral lymph nodes (LNs), and the white pulp of the spleen. They participate in T-cell–dependent immune responses and immunologic memory [14]. MZB cells ($B220^{+}/CD23^{low}/CD21^{high}$) are derived from circulating progenitors, but when they arrive to the spleen, they locate in the marginal zone and do not recirculate; they have been shown to capture blood-borne antigens and deliver them to dendritic cells (DCs) of the follicular areas [15]. Also, activated MZB cells can migrate to the T-B border and directly induce the expansion of antigen-specific T cells [16].

Prompted by the central role of B cells in autoimmune diseases [17–19] and by the successful induction of *in vitro* T-cell responses using tumor antigen–pulsed, CD40-activated B cells [20,21], we investigated the role of B cells in brain tumor regression induced by intratumoral treatment with Ad-TK+Ad-Flt3L. Using KO mice that lack B cells and specific antibodies that deplete total B cells or MZB cells, we found that, in the absence of B cells, Ad-TK+Ad-Flt3L fails to induce the regression of intracranial GBM. Tumor antigen–specific T-cell clonal expansion was also abolished in B-cell–deficient mice ($Igh6^{-/-}$), indicating that functional, mature B cells were required for mounting a systemic immune response against brain tumor antigens. The role of B cells in this antitumor immune response does not, however, seem to be mediated by the production of antitumor-specific antibodies because we could not detect evidence of humoral antitumor immunity and the treatment was still efficacious in mice deficient in plasma cells formation, $Prdm^{flox/flox}CD19^{Cre/+}$ mice. Although the most evident function of B cells in adaptive immune responses is the clonal differentiation of antigen-specific B cells into plasma cells and the subsequent secretion of antigen-specific immunoglobulin (Ig), B cells can also function as efficient APCs [9,17,20–22]. Ad-Flt3L/Ad-TK treatment induced an increase in the levels of B cells in the cervical LNs of WT mice. These B cells contained brain tumor remnants, increased expression of coactivation markers, and induced the clonal expansion of syngeneic tumor antigen–specific T lymphocytes. Taken together, our results imply that B cells may act as APCs to enhance clonal expansion of tumor antigen–specific T lymphocytes and T cell–dependent tumor regression within the central nervous system.

Materials and Methods

Ads

First-generation, E1/E3–deleted replication-deficient recombinant adenovirus serotype 5 was used in this study. We used Ad-Flt3L [3] and Ad-TK [3]; both transgenes are under the control of human CMV promoter. An Ad without a transgene was used as a control (Ad-0). All viral preparations were confirmed to be replication competent adenovirus and lipopolysaccharide (LPS) free. Viral titers were determined by an end-point dilution cytotoxic-effect assay. The methods for Ad generation, purification, characterization, and scale-up have been

previously described by our laboratory [3]. Ads were administered within the intracranial tumors as described below using the following doses: Ad-TK, 10^8 infectious units (iu); Ad-Flt3L, 2×10^8 iu; and Ad.0, 3×10^8 iu (to deliver equivalent total iu).

Mouse Glioma Models

Female C57BL/6 wild-type mice, green fluorescent protein ($GFP^{+/+}$) mice, and $Igh6^{-/-}$ on C57BL/6 background were purchased from Jackson Laboratories (Bar Harbor, ME). Inbred VM/Dk mice were donated by the McLaughlin Research Institute (Great Falls, MT) and bred in the CSMC vivarium. $Prdm1^{flox/flox}$ $CD19^{Cre/+}$ mice that lack Blimp-1 in B cells were generated as previously described [23] by crossing mice expressing Cre-recombinase under the control of the CD19 promoter ($CD19^{Cre/+}$) [23] with $Prdm1^{flox/flox}$ mice, which have the *prdm-1* locus encoding Blimp-1 flanked by loxP sites [23]. Experimental mice used in this study were of $Prdm1^{flox/flox}CD19^{Cre/+}$ genotype. Both the $CD19^{Cre/+}$ and the $Prdm1^{flox/flox}$ mice were backcrossed to C57BL/6J 10 times before mating to generate $Prdm1^{flox/flox}$ $CD19^{Cre/+}$. Intracranial GBM models were generated as previously described [2,24]. Mice were stereotactically injected with GBM cells (either 20,000 GL26 cells, 20,000 GL26-OVA cells [24] [stably expressing cytoplasmic chicken ovalbumin], or 5000 SMA-560 cells [25], a gift from Darell Bigner [Duke University]), in a volume of 1 μl into the right striatum (+0.5 mm anterior-posterior, +2.1 mm medial-lateral, and −3.2 mm dorsoventral from bregma). Fourteen days later, vectors were administered intratumorally using the same burr hole (at −2.9, −3.2, and −3.5 mm DV from bregma: 0.5 μl per site). Ganciclovir (GCV, 25 mg/kg per day) was administered intraperitoneally (i.p.) for 7 days after vector administration to all animals receiving Ad-TK. To assess whether B cells are involved in the memory response elicited by the combined conditional cytotoxic/immune gene therapy, mice were rechallenged by injection of 20,000 tumor cells in the contralateral brain hemisphere [2]. Mice were killed at specific time points or when their health status reached criteria established by the guidelines of the Institutional Animal Care and Use Committee at Cedars-Sinai Medical Center (approved protocol 2259). Mice were killed under deep anesthesia by terminal perfusion with oxygenated, heparinized Tyrode solution. Blood, cervical LNs, spleen, and tumors were collected immediately after perfusion and processed for flow cytometric analysis or ELISA. When brains were analyzed by immunofluorescence, mice were also perfused with 4% paraformaldehyde (PFA) in phosphate-buffered saline (PBS), and brains were postfixed in 4% PFA for three additional days.

Generation of Bone Marrow Chimeric Mice

Bone marrow chimeric mice were generated using $GFP^{+/+}$ and wild-type C57BL/6 mice as described by us previously [2]. Briefly, irradiated recipient mice (7 Gy) were adoptively transferred with 10^7 bone marrow cells from donor mice through tail vein injection. Bone marrow in the recipients was allowed to reconstitute for 10 weeks before intracranial implantation of GL26 tumor cells. Tumor-infiltrating immune cells were purified using Percoll gradient centrifugation as described below. The origin of tumor-infiltrating B cells ($CD19^+$/$CD45^+$) was determined by analyzing their relative expression of GFP by flow cytometry.

B-Cell Depletion Experiments

B-cell depletion. The IgG2a 18B12 monoclonal antimouse CD20 antibody was generated as previously described [26]. The IgG2a mouse antihuman 2B8 CD20 monoclonal antibody was used as isotype control [26]. The duration of B-cell depletion was assessed in naive mice injected i.p. with 300 μl of 1 mg/ml antimouse CD20 or isotype control. B-cell content and integrity of T-cell populations were determined by flow cytometry in spleen 7 or 12 days later. The integrity of T-cell populations in B-cell–depleted mice was determined 7 days after depletion using the following antibodies: hamster antimouse CD3ε, rat antimouse CD8α, and rat antimouse CD4 (Table W1). GL26 tumor-bearing mice were injected i.p. with antimouse CD20 on the day of the treatment with Ad vectors and again 2 weeks later to maintain depletion. Animals undergoing rechallenge experiments received i.p. injections of depleting antibodies on the day of the rechallenge (day 90) and 2 weeks later (day 105).

MZ B-cell depletion. MZB cells were depleted with 100 μg of anti–LFA-1 and 100 μg of anti-CD49d [27]. To assess the duration of MZB cell depletion, naive mice were injected with these antibodies or isotype controls (Table W1). The content of MZB cells was determined by flow cytometry in the spleen 3, 7, and 10 days later. The integrity of T-cell populations in MZB cell–depleted mice was determined 7 days after depletion using the antibodies indicated above. GL26 tumor-bearing mice were injected i.p. with anti–LFA-1 and CD49d or isotype controls on the day of the treatment with Ad vectors and 10 days later.

Isolation and Characterization of Immune Cells in Brain Tumor, Spleen, and Cervical LNs

Brains were carefully separated from the meninges and removed from the skull. The tumor was dissected, taking care to avoid the ventricles. Tumors were homogenized in RPMI medium using a glass Tenbroeck homogenizer (Kontas Glass Company). To purify mononuclear cells from the tumor, homogenized tumor tissue was centrifuged through a Percoll (GE Healthcare, Piscataway, NJ) step gradient (70%-30% Percoll in PBS) for 20 minutes at 2200 RPM. Immune cells were extracted from draining cervical LNs by homogenization using a Tenbroeck homogenizer. Splenocytes were collected by homogenization of whole spleen followed by incubation in red blood cell lysis buffer ACK (0.15 mM NH_4Cl, 10 mM $KHCO_3$, and 0.1 mM sodium EDTA at pH 7.2) for 3 minutes on ice. Immune cells were counted and labeled with the rat IgGs (BD Pharmingen, San Diego, CA) depicted in Table W1 and dissolved in 1% FBS–0.1 M PBS. Samples were analyzed using a FACScan Flow cytometer (Beckton Dickinson, Franklin Lakes, NJ) and Summit software (Cytomation, Inc, Fort Collins, CO).

Immunofluorescence

Coronal sections of PFA-fixed brains (50 μm) were obtained using a Leica vibratome (Leica Microsystems Heidelberg, Mannheim, Germany). Sections were incubated in 10 mM citrate (60°C) for antigen retrieval, and immunofluorescence was performed using the antibodies described in Table W1. Nuclei were stained with 4′, 6-diamidino-2-phenylindole (DAPI, 5 μg/ml; Invitrogen, Carlsbad, CA), and tissues were mounted with ProLong Antifade (Invitrogen). Confocal micrographs were obtained using a Leica confocal microscope TCS SP2 with AOBS equipped with 405-nm violet-diode UV laser, 488-nm argon laser, and 594-helium-neon lasers and using a HCX PL APO 63× 1.4 numerical aperture oil objective (Leica Microsystems Heidelberg, Mannheim, Germany) [28].

Detection of Total IgG

Homogenized splenocytes were collected followed by incubation in red blood cell lysis buffer ACK and then incubated with RPMI

alone or in the presence of LPS (10 μg/ml) for 72 hours. After activation, total IgG levels were determined in 20 μl of cell culture supernatants using the Easy-Titer Mouse IgG Kit (Pierce, Rockford, IL) following the manufacturer's instructions.

Detection of Circulating Antitumor Antibodies

Detection of circulating antitumor antibodies was performed in mouse serum collected 7 days after Ad-TK+Ad-Flt3L treatment as previously described [4]. Briefly, cultured GL26, GL26-OVA, and SMA-560 cells were stained with rat antimouse IgM-fluorescein isothiocyanate (FITC, 1:50, 553437; BD Pharmingen) or antimouse IgG-FITC (1:1000, A-11017; Invitrogen). Samples were analyzed using a FACScan flow cytometer (Beckton Dickinson).

Flt3L ELISA

Detection of Ad-derived human Flt3L and endogenous mouse Flt3L was performed in serum 7 days after vector injection. Serum was diluted 1:10 in Dulbecco PBS. The expression of human and mouse Flt3L was determined using species-specific ELISA kits (DFK00 and MFK00; R&D Systems).

Trafficking of CellTracker Green–Labeled Tumor Antigen

Cells were labeled with CellTracker Green as described previously [2]. Briefly, 10^7 GL26 cells were labeled with CellTracker Green (4 μM). A total of 250,000 cells in 1.5 μl were injected in the brain striatum of C57BL/6 mice. Mice were treated 2 days later by intratumoral injection of saline or Ad-Flt3L and Ad-TK, and tumor-infiltrating immune cells and cervical-draining LNs were harvested 2 and 7 days later and processed for flow cytometry.

Syngeneic Mixed Leukocyte Reaction

B cells were purified from the cervical LNs of GL26-OVA tumor-bearing mice 7 days after the treatment with Ad-TK+Ad-Flt3L or saline using a pan B-cell isolation kit (130-095-813; Miltenyi Biotec, Bergisch Gladbach, Germany) in an OctoMACS Separator (Miltenyi Biotec). The purity of B-cell preparations was more than 95%, as determined by flow cytometry using antibodies against mouse CD45, mouse CD19, mouse CD14, and mouse CD3ε (Table W1). Enriched B-cell preparations were incubated with 2 μg/ml $OVA_{323-339}$, a known H-2^b–restricted OVA class II epitope [29] for 3 hours at 37°C, followed by incubation with 50 μg/ml mitomycin C for 30 minutes at 37°C to inhibit the proliferation of B cells in the syngeneic mixed leukocyte reaction (MLR). Splenocytes were collected from naive OT-II mice, donated by Dr Jonathan Kaye (Gene Therapeutics Research Institute; Cedars-Sinai Medical Center). The syngeneic MLR was performed by incubating 200,000 OT-II splenocytes in the presence of increasing ratios of B cells (1:16, 1:8, 1:4, 1:2, and 1:1) for 90 hours. Cell proliferation was determined by the incorporation of BrdU into nascent DNA strands and assessed by ELISA (BrdU Cell Proliferation Assay, catalog no. 11647229001; Roche, Mannheim, Germany).

Interferon γ ELISPOT

C57BL/6 mice and Igh6$^{-/-}$ mice were implanted with GL26 tumor cells and treated 14 days later with Ads expressing Ad-Flt3L and Ad-TK or saline. Mice were killed 7 days later, and splenocytes were collected as described previously. A total of 1×10^5 splenocytes were plated in triplicate onto a capture anti–interferon γ (IFNγ) antibody–coated (1:60; R&D Systems, Minneapolis, MN) 96-well ELISPOT plate (polyvinylidene fluoride; Millipore, Billerica, MA), and IFNγ secretion was quantified according to the manufacturer's protocol. Briefly, 1×10^5 splenocytes were stimulated for 24 hours at 37°C in RPMI 1640 medium with or without 1 μg/ml $Trp2_{180-188}$ peptide (Sigma, Milwaukee, WI). ConA (1 μg/ml, 4 hours) stimulation of splenocytes served as a positive control. Plates were vigorously washed with PBS before incubation with IFNγ detection antibody (1:60; R&D Systems). Twenty-four hours later, plates were developed after incubation with streptavidin–horseradish peroxidase (R&D Systems) and visualized by amino ethyl carbazole (Sigma-Aldrich). Spots were detected and counted using the KS ELISPOT (version 4.7; Zeiss, Göttingen, Germany).

Statistical Analysis

Sample sizes were calculated to detect differences between groups with a power of 80% at a 0.05 significance level using PASS 2008 (Power and sample size software; NCSS, Kaysville, UT). Kaplan-Meier survival curves were analyzed using the Mantel log-rank (GraphPad Prism version 3.00; GraphPad Software, San Diego, CA). One- or two-way analysis of variance (ANOVA) followed by the Tukey test or unpaired two-tailed Student's *t* test (NCSS) were used to analyze ELISPOT, ELISA, and flow cytometry data, as indicated in the figure legends. When data failed normality test or Levene equal-variance test, they were square root transformed. Curve inequality in MLR experiments was assessed using the randomization test (NCSS). $P < .05$ was considered the cutoff for significance. All experiments were performed at least twice to confirm the findings.

Results

Bone Marrow–Derived B Cells Infiltrate Intracranial Brain Tumors and Are Required for Antitumor Immunity and Tumor Regression In Vivo

Our previous results show that intratumoral administration of Ad-Flt3L/Ad-TK leads to a T-cell–dependent antitumor immune response that induces tumor regression in rodent models of glioblastoma [3,4]. Considering that the role of B cells in anti-brain tumor immunity remains elusive, we aimed to investigate whether B cells play a role in the generation of adaptive immune responses against brain tumor antigens (Figure 1*A*).

Using immunofluorescence techniques followed by confocal microscopy, we detected CD19$^+$ cells within the brain tumor mass in C57BL/6 bearing syngeneic GL26 tumors (Figure 1*B*). These findings are in agreement with the fact that B cells have been found to infiltrate GBM in humans [30]. To investigate whether the CD19$^+$ cells that infiltrate the tumor originate from the bone marrow or from the central nervous system, we generated bone marrow chimeric mice consisting of bone marrow from wild-type C57BL/6 mice adaptively transferred into irradiated GFP$^{+/+}$ mice. We found that only 17.5% of tumor-infiltrating B cells in chimeric mice were GFP+, which was only slightly higher than the background observed in WT mice (8% GFP+ B cells). Therefore, our data suggest that most of the CD19$^+$ infiltrating immune cells in Ad-TK+Ad-Flt3L–treated brain tumors are bone marrow derived (Figure 1*C*).

We next evaluated whether B cells are required to induce the antitumor immune response triggered by the treatment with Ad-TK+Ad-Flt3L. We implanted GL26 tumor in the brain of Igh6$^{-/-}$ mice, which are deficient in mature B cells, and treated them 14 days later with Ad-TK+Ad-Flt3L, or saline as a control (Figure 1, *D* and *E*). Whereas in wild-type mice, treatment with Ad-TK+Ad-Flt3L induced tumor regression and long-term survival in 60% of the animals, the treatment failed in Igh6$^{-/-}$ mice (Figure 1*D*). Tallying with these findings, we

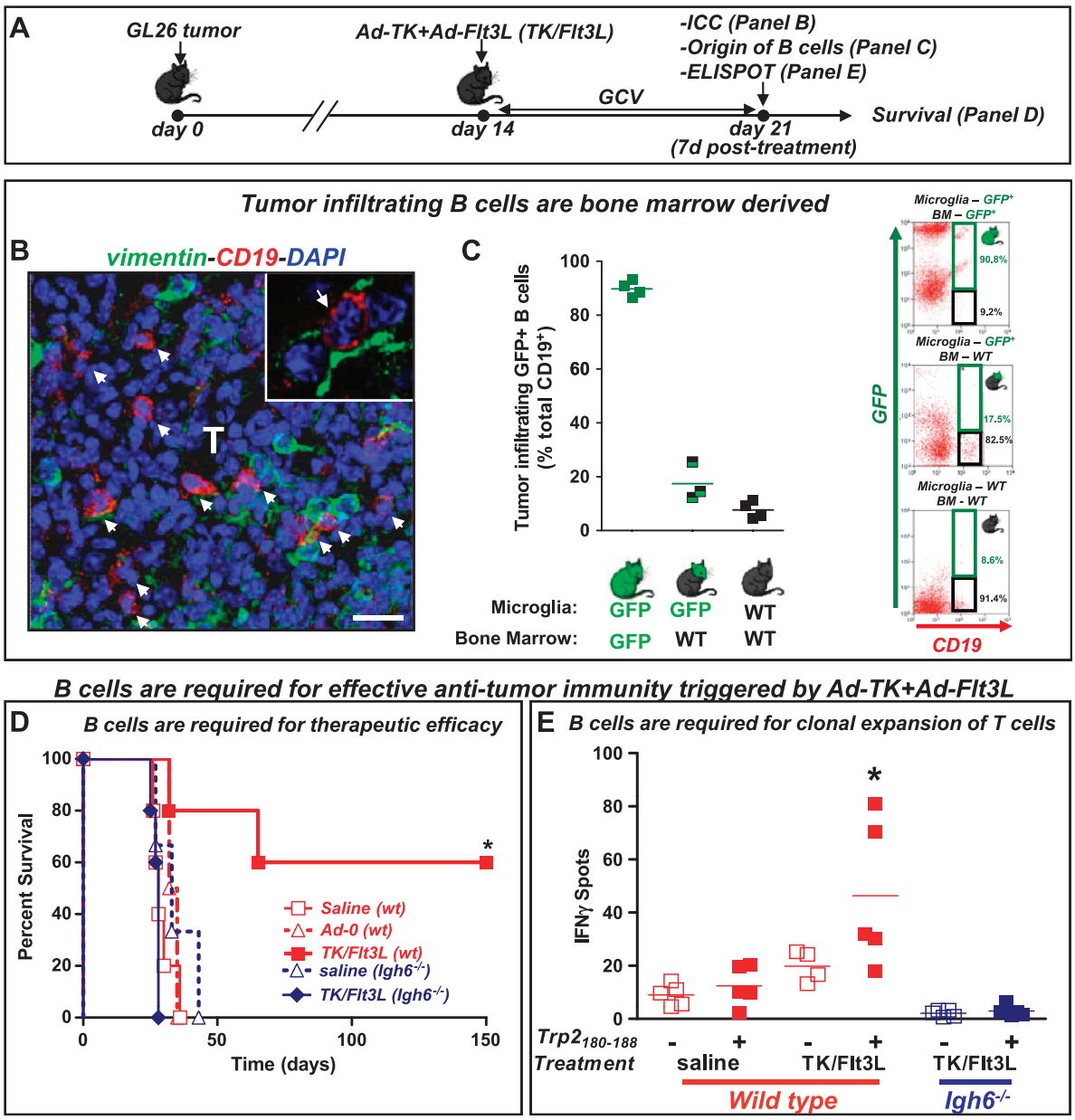

Figure 1. Bone marrow–derived B cells infiltrate into tumors and are required for tumor regression. (A) GL26 cells were implanted in the striatum of wild-type (WT) or Igh6$^{-/-}$ C57BL/6 mice. Mice were treated 14 days later with an intratumoral injection of Ad-TK+Ad-Flt3L (TK/Flt3L), and as controls, with saline or an empty vector (Ad.0). (B) Representative confocal image shows B cells (CD19, red) infiltrating the tumors (vimentin, green) 7 days after the treatment. Nuclei were stained with 4′, 6-diamidino-2-phenylindole (blue). Arrows indicate tumor-infiltrating B cells. Scale bar, 20 μm. (C) Chimeric mice were constructed to assess the origin of CD19^{+} B cells infiltrating into the tumor. WT mice were irradiated and reconstituted with bone marrow from transgenic GFP$^{+/+}$ mice. WT, GFP$^{+/+}$, and chimeric mice were implanted with intracranial GL26 tumors 10 weeks after irradiation and treated with Ad-TK+Ad-Flt3L 14 days later. Seven days after the treatment, tumor-infiltrating GFP^{+} B cells were quantified by flow cytometry. Representative dot plots show tumor-infiltrating GFP^{+} B cells (GFP^{+}, CD19^{+}; green boxes) or GFP^{-} B cells (GFP^{-}, CD19^{+}; black boxes), gated for CD45^{+} live leukocytes. (D) Kaplan-Meier survival curves show efficacy of Ad-TK+Ad-Flt3L. *$P < .05$ *versus* saline. Mantel log-rank test. (E) Splenocytes were isolated from wild-type or Igh6$^{-/-}$ mice 7 days after treatment. Cells were incubated with or without Trp2$_{180\text{-}188}$, a GL26 tumor antigen. The frequency of IFNγ-secreting T cells was assessed by ELISPOT. *$P < .05$ *versus* without Trp2$_{180\text{-}188}$ (two-way ANOVA followed by the Tukey test).

did not observe an increase in the frequency of T-cell precursors that released IFNγ in response to tumor antigen (Trp2$_{180\text{-}188}$, a known GL26 H-2K^{b}–restricted tumor antigen) in Igh6$^{-/-}$ mice implanted with GL26 tumors and treated with Flt3L and TK (Figure 1*E*). Thus, our results suggest that B cells mediate clonal expansion of tumor antigen–specific T cells and subsequent brain tumor regression.

Considering that Igh6$^{-/-}$ mice may display other immunologic defects [31] in addition to the lack of mature B cells, we aimed to substantiate these initial findings by depleting B cells from tumor-bearing wild-type animals. We first depleted B cells using an antimouse CD20 antibody [26]. CD20 is a B-cell–specific molecule that is first expressed on the cell surface during the pre-B to immature B-cell transition but

is lost on plasma cell differentiation [32]; administration of CD20 antibodies does not deplete plasma cells [32]. Administration of anti-mCD20 to naive mice led to more than 95% depletion of B cells for at least 3 weeks (Figure 2*A*) but did not reduce the population of $CD8^+$ or $CD4^+$ T cells in the spleen (Figure W1). Thus, anti-mCD20 was administered to tumor-bearing mice on the day of treatment, and again 2 weeks later. B-cell depletion did not affect tumor progression in saline-treated mice, but it severely impaired the efficacy of Ad-TK+Ad-Flt3L, confirming a critical role for B cells in mediating the antitumor immune response induced by this treatment (Figure 2*B*). Because Ad-TK+Ad-Flt3L gene therapy induces immunologic memory against the tumor [2], we investigated whether B cells are involved in the memory response elicited. We implanted Ad-TK+Ad-Flt3L–treated long-term survivors with GL26 glioma cells in the contralateral brain hemisphere and mice did not receive further treatment, except for the administration of depleting anti-mCD20 (Figure 2*C*). B-cell depletion led to significant reduction in the survival of rechallenged mice, suggesting that B cells play an important role in the antitumor immunologic memory induced by Ad-TK+Ad-Flt3L.

Using flow cytometry analysis, we assessed the content of B cells ($CD45^+/B220^+$) in the spleen of tumor-bearing mice. We did not find significant changes in the level of B cells when comparing treated

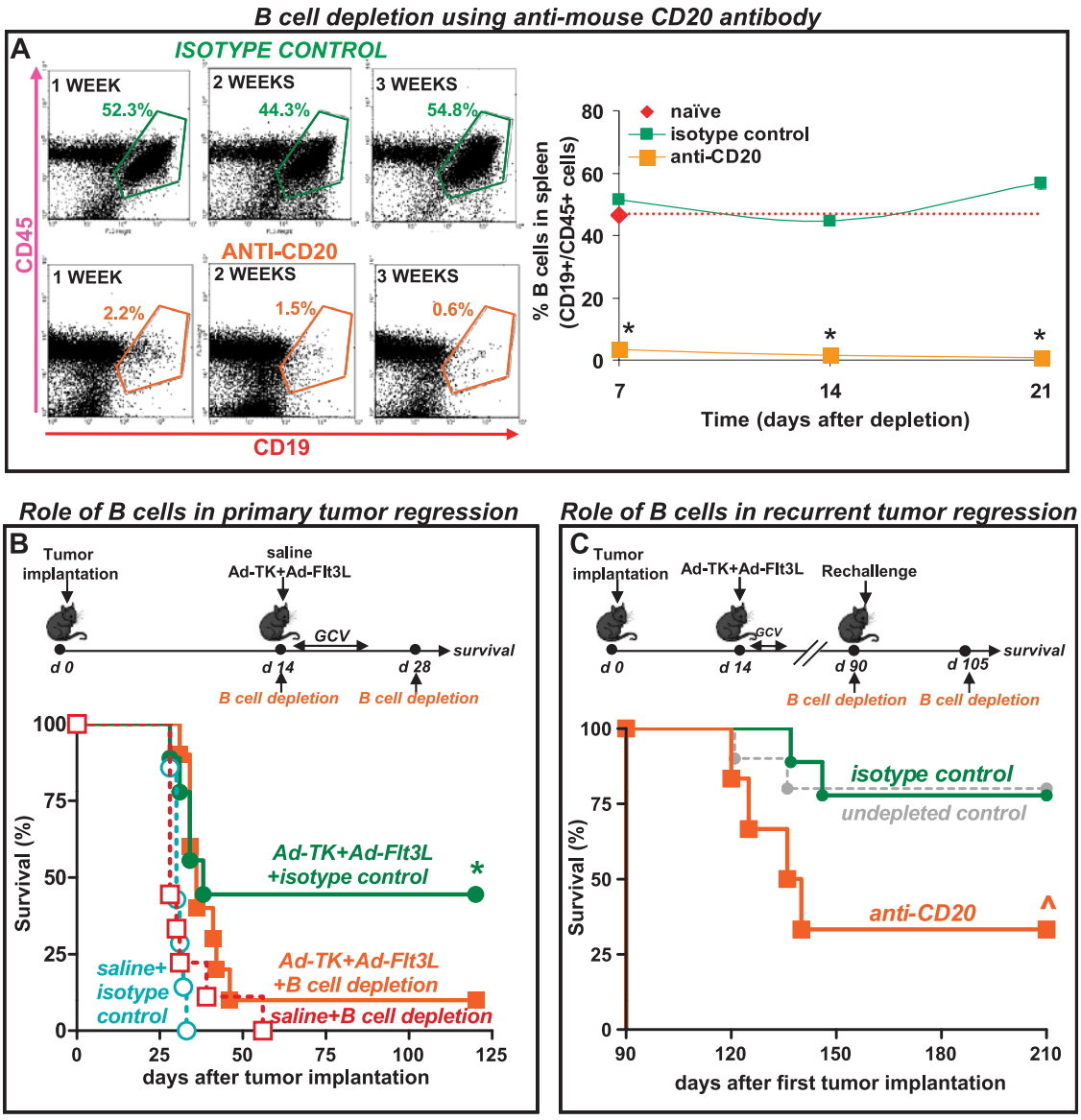

Figure 2. B-cell depletion impairs the efficacy of the immunotherapy. (A) Representative dot plots show efficacy of $CD20^+$ cell depletion in naive mice injected i.p. with mouse antimouse CD20 antibody (IgG2a, 300 μg) or with isotype control (mouse anti-human CD20 IgG2a, 300 μg). Spleens were collected 7, 14, and 21 days after depletion and B cells ($CD45^+/CD19^+$) were quantified by flow cytometry. *$P <$ .05 *versus* isotype control (two-way ANOVA). (B) GL26 cells were implanted in the striatum of C57BL/6 mice and treated 14 days later with an intratumoral injection of Ad-TK+Ad-Flt3L or saline. B-cell depletion was performed at days 14 and 28 after tumor implantation. Kaplan-Meier survival curves show efficacy of Ad-TK+Ad-Flt3L–treated animals. *$P <$ .05 *versus* saline. Mantel log-rank test. (C) Ad-TK+Ad-Flt3L–treated wild-type C57BL/6 mice that survived a first intracranial tumor were implanted in the contralateral striatum with GL26 tumor cells 90 days later. B cells were depleted by i.p. injection of mouse anti-CD20 antibody or isotype control on the day of the rechallenge and 2 weeks later. ^$P <$ .05 *versus* isotype control. Mantel log-rank test.

versus control mice (data not shown). However, when we assessed the levels of MZB cells ($B220^+/CD21^+/CD23^-$), we found that treatment with Ad-TK+Ad-Flt3L induced a rapid increase in the levels of MZB cells in the spleen 7 days after the treatment (Figure 3*A*); MZB cells returned to normal levels by day 12 after treatment. In view of these findings, we aimed to evaluate the role of MZB cells in the antitumoral effect of Ad-TK+Ad-Flt3L treatment. MZB cells were depleted using antibodies against LFA-1 and CD49d [27,33]. At 3 and 10 days after administration in naive mice, these antibodies depleted 95% and 85% of MZB cells, respectively (Figure 3*B*), but did not affect the levels of $CD4^+$ or $CD8^+$ T-cell populations in the spleen (Figure W1). Whereas MZB cell depletion did not affect tumor progression in saline-treated mice, it abrogated the antitumor activity of Ad-TK+Ad-Flt3L, suggesting that MZB cells play a critical role in the antitumor immune response induced by the treatment (Figure 3*C*).

Effect of B Cells on Ad-TK+Ad-Flt3L–Induced Antitumor Immunity Is Not Mediated by the Production of Antitumor Antibodies

Considering that an important function of B cells is to produce antibodies against specific antigens, we next examined whether Ad-TK+Ad-Flt3L induces a specific, humoral anti-brain tumor immune response. Therefore, we collected serum from GL26 tumor-bearing mice and assessed the presence of circulating antitumor antibodies by flow cytometry (Figures 4 and W2). We did not find detectable levels of anti-GL26 circulating IgM or IgG at either day 7 or day 12 after the treatment. Also, we did not observe an antitumor humoral immune response when we assessed the presence of anti–GL26-OVA antibodies in the serum of GL26-OVA–bearing mice on treatment with Ad-TK+Ad-Flt3L, when compared with Ad.0 or saline-treated control mice (Figure W3).

To rule out that the lack of antitumor humoral immunity was strain related, we used an additional intracranial tumor model. Inbred VM/Dk mice were implanted in the brain with SMA-560 cells [25] and treated 12 days later with gene therapy. Whereas all the mice that received saline or single treatments succumbed to tumor burden by day 30, Ad-TK+Ad-Flt3L treatment led to long-term survival in 50% of the mice (Figure 4*C*). However, when we assessed the presence of circulating anti-SMA-560 antibodies 7 days after the treatment, we did not find detectable levels of anti–SMA-560 IgM (Figure 4*D*) or IgG (Figure 4*E*).

To more conclusively establish that the role of B cells in the efficacy of Ad-TK+Ad-Flt3L is not mediated by the production of antibodies, we used an additional KO mouse model in which B cells cannot differentiate to plasma cells and thus cannot produce IgGs, that is, $Prdm1^{flox/flox}$ $CD19^{Cre/+}$ mice that lack Blimp-1 specifically in B cells. In agreement with previous reports [23], B cells purified from the spleen of $Prdm1^{flox/flox}$ $CD19^{Cre/+}$ mice were incapable of immunoglobulin secretion and expression of CD138 on *in vitro* stimulation with LPS (Figure 5*A*). We found that Ad-TK+Ad-Flt3L led to 50% long-term survival in both wild-type and $Prdm1^{flox/flox}$ $CD19^{Cre/+}$ mice (Figure 5*B*), suggesting that plasma cells are not required for the efficacy of this treatment and that the role of B cells in the antitumor immune response does not involve the production of antibodies in this model.

B Cells Containing Tumor Cell Remnants Are Present in the Draining LNs after Treatment with Ad-TK+Ad-Flt3L

Because we established that Ad-TK+Ad-Flt3L efficacy is dependent on B-cell function but does not require the production of antitumor immunoglobulins, we hypothesized that B cells could be acting as APCs. Because it had been shown that Flt3L can expand B-cell populations [34,35], we assessed whether Ad-derived Flt3L expressed in the tumor mass could reach the peripheral circulation and cause an increase of B cells in the dLN. We detected circulating transgenic Flt3L (human) within the tumor mass and in the serum of tumor-bearing mice 7 days after treatment with Ad-TK+Ad-Flt3L (Figure W4).

We next assessed the content and activation status of B cells in the cervical LNs of GL26 tumor-bearing mice. B-cell levels increased in the cervical LNs 7 days after intratumoral delivery of Ad-TK+Ad-Flt3L when compared with control mice (Figure 6*A*). To assess the activation status of B cells in the draining LNs, we evaluated the expression levels of costimulatory molecules CD40 and CD86. Seven days after the treatment with Ad-TK+Ad-Flt3L, the percentage of both $CD40^+$ (Figure 6*B*) and $CD86^+$ (Figure 6*C*) B cells increased in the cervical LNs compared with control mice, indicating that B cells were activated in response to the intratumoral delivery of Ad-TK+Ad-Flt3L.

B cells can capture and present antigen [36,37] directly to T cells through MHC I [38,39] and II [9,40] after the up-regulation of coactivation markers on their cell surface [41]. To investigate the possible role of B cells as APCs in our model, i.e., functioning as brain tumor APCs *in vivo*, GL26 tumor cells were labeled with fluorescent CellTracker Green and were implanted in the brain striatum. We then quantified the total number of B cells in the tumor and in the draining LNs that were associated with CellTracker Green–labeled tumor antigen. A subpopulation of tumor-infiltrating B cells (~200 cells) from saline-treated animals were labeled with CellTracker Green, suggesting that they had become associated with GL26 tumor cell antigens (Figure 6*D*). Interestingly, a significant increase (two-fold, $P < .05$) in the number of tumor-infiltrating B cells associated with tumor antigen (~400 cells) was observed in TK/Flt3L–treated animals (Figure 6*D*). We also found that treatment with Ad-TK+Ad-Flt3L induced a significant increase in the number of B cells associated with CellTracker Green–labeled tumor cell remnants in the cervical draining LNs (Figure 6*E*), and although in isolation, this finding does not provide direct evidence for the role of B cells in antigen uptake and presentation; it demonstrates that B cells have the ability to engulf tumor antigen and transport it to T-cell–rich areas.

B Cells Isolated from the dLN of Ad-Flt3L+Ad-TK–Treated Animals Stimulate T-cell Proliferation

Up-regulation of activation markers on B cells is required to induce proliferation of antigen-specific T lymphocytes [42]. We hypothesized that the expression of activation markers in a subset of B cells could stimulate the proliferation of syngeneic T cells. As such, we performed a syngeneic, antigen-specific MLR. We sort-purified B cells ($CD45^+/CD19^+$) from the cervical LNs of GL26-OVA tumor-bearing mice 7 days after treatment with Ad-Flt3L/Ad-TK or saline (Figure 7*A*). Considering the small number of B cells loaded with tumor antigen present in the LNs of treated mice (~400 cells; Figure 6*D*), we first pulsed them with the OVA peptide presented in the context of MHC-II ($OVA_{323-339}$) to amplify the signal to be detected by this assay. B cells were then cocultured with splenocytes from naive OT-II transgenic mice, which have a T-cell receptor specific for $OVA_{323-339}$ in the context of $I\text{-}A^b$. B cells isolated from the LNs of Ad-TK+Ad-Flt3L–treated mice significantly increased the proliferation of OT-II splenocytes when compared with B cells from saline-treated control mice (Figure 7, *B* and *C*).

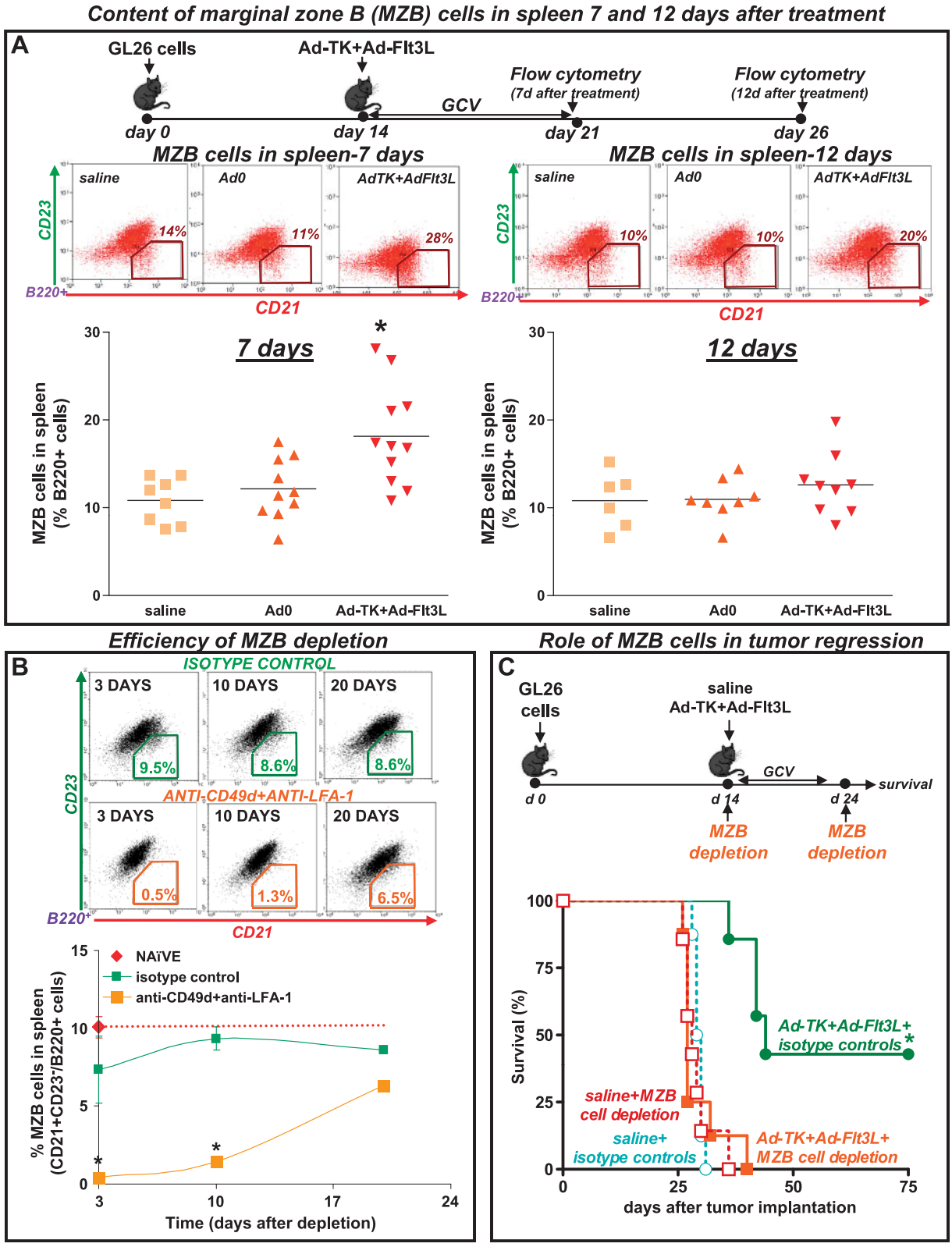

Figure 3. MZB cell depletion impairs the efficacy of the immunotherapy. (A) GL26 cells were implanted in the striatum of wild-type C57BL/6 mice. Mice were treated 14 days later with an intratumoral injection of Ad-TK+Ad-Flt3L, and as controls, with saline or an empty vector (Ad.0). At 7 and 12 days after the treatment, levels of MZB cells in the spleen were quantified by flow cytometry using anti-B220, anti-CD21, and anti-CD23 antibodies. *$P < .05$ *versus* saline, ^$P < .05$ *versus* Ad.0. (B) Representative dot plots show efficacy of MZB cell depletion in the spleen of naive mice 3, 10, and 20 days after i.p. administration of anti-CD49d antibody (100 μg) and anti-LFA-1 antibody (100 μg) or the corresponding isotype controls (rat IgG2a and rat IgG2b, 100 μg each). *$P < .05$ *versus* isotype control (two-way ANOVA). (C) GL26 cells were implanted in the striatum of C57BL/6 mice and treated 14 days later with an intratumoral injection of Ad-TK+Ad-Flt3L or saline. MZB cell depletion was performed at days 14 and 24 after tumor implantation. Kaplan-Meier survival curves show efficacy of Ad-TK+Ad-Flt3L–treated animals. *$P < .05$ *versus* saline. Mantel log-rank test.

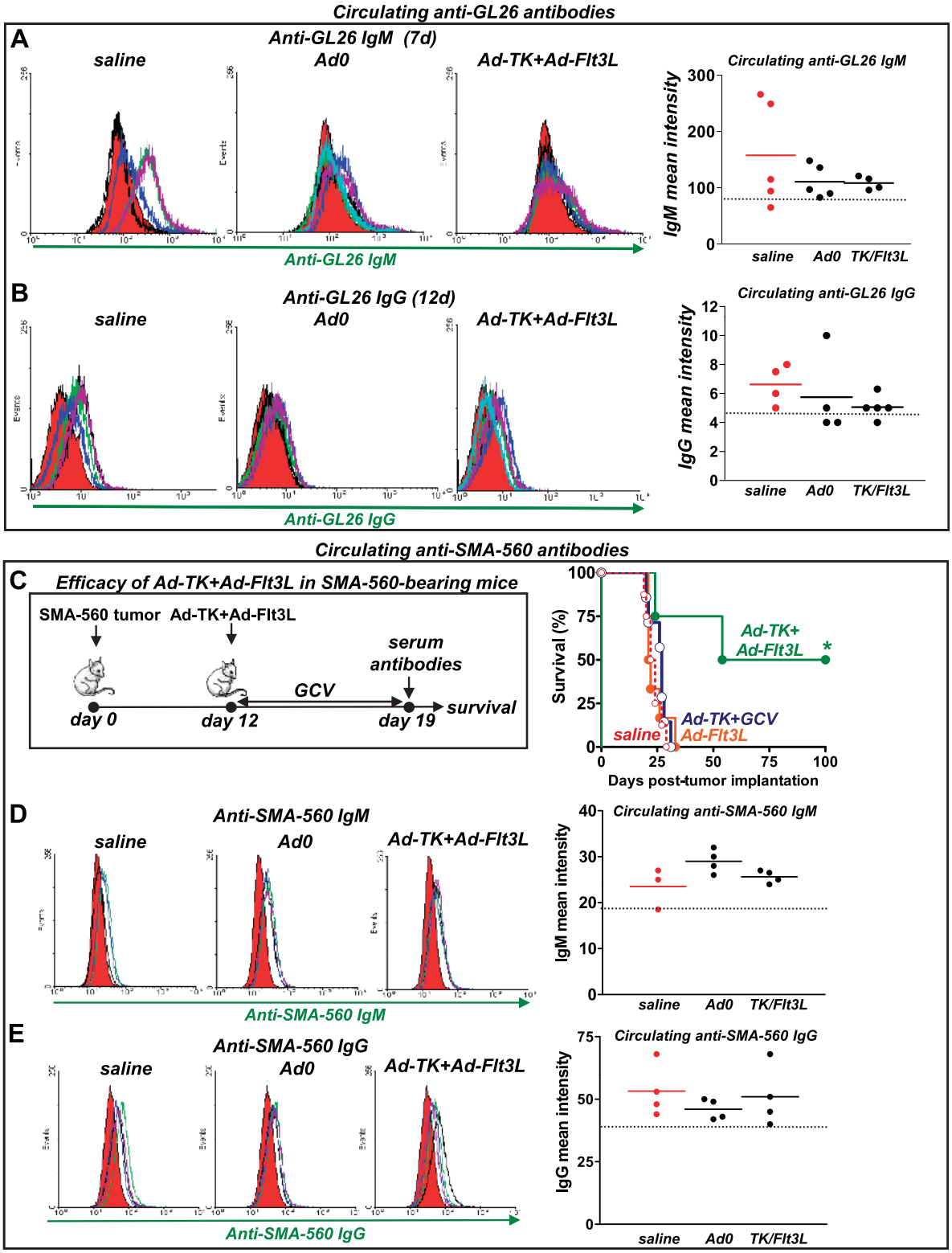

Figure 4. Assessment of the antibody response against the tumor. (A and B) GL26 cells were implanted in the striatum of C57BL/6 mice and treated 14 days later with an intratumoral injection of Ad-TK+Ad-Flt3L, saline, or an empty vector (Ad.0). At 7 (A) and 12 (B) days after the treatment, serum was collected to evaluate the presence of circulating anti-GL26 cell IgM (A) and IgG (B), respectively. Histograms and graphs show the fluorescence intensity of fixed GL26 cells that were incubated with normal C57BL/6 serum (red area) or serum from treated tumor-bearing mice (colored lines), followed by FITC-conjugated antimouse IgM or IgG. (C) Kaplan-Meier survival curves show the survival of inbred VM/Dk mice bearing intracranial SMA-560 tumors and treated 12 days later with Ad-TK+Ad-Flt3L, saline, or Ad.0. *$P < .05$ *versus* saline (log-rank test). Seven days after the treatment, serum was collected to evaluate the presence of circulating anti–SMA-560 cell antibodies. (D and E) Histograms and graphs show the fluorescence intensity of fixed SMA-560 cells that were incubated with normal inbred VM/Dk mouse serum (red area) or serum from treated mice (colored lines), followed by FITC-conjugated antimouse IgM (D) or FITC–antimouse IgG (E).

Discussion

In the present study, we investigated the role of B cells in the immune response induced by Ad-TK+Ad-Flt3L against brain tumors. Whereas the role of T cells in the clearance of brain and peripheral tumors has been extensively studied, the involvement of B cells in antitumor immunity is poorly understood. We demonstrated that B cells are recruited into the brain tumor microenvironment after treatment with Ad-TK+Ad-Flt3L and that they can collect antigen, transport it to the draining LNs, and present it to T cells, playing a critical role as APCs in the immune response against tumors located within the brain.

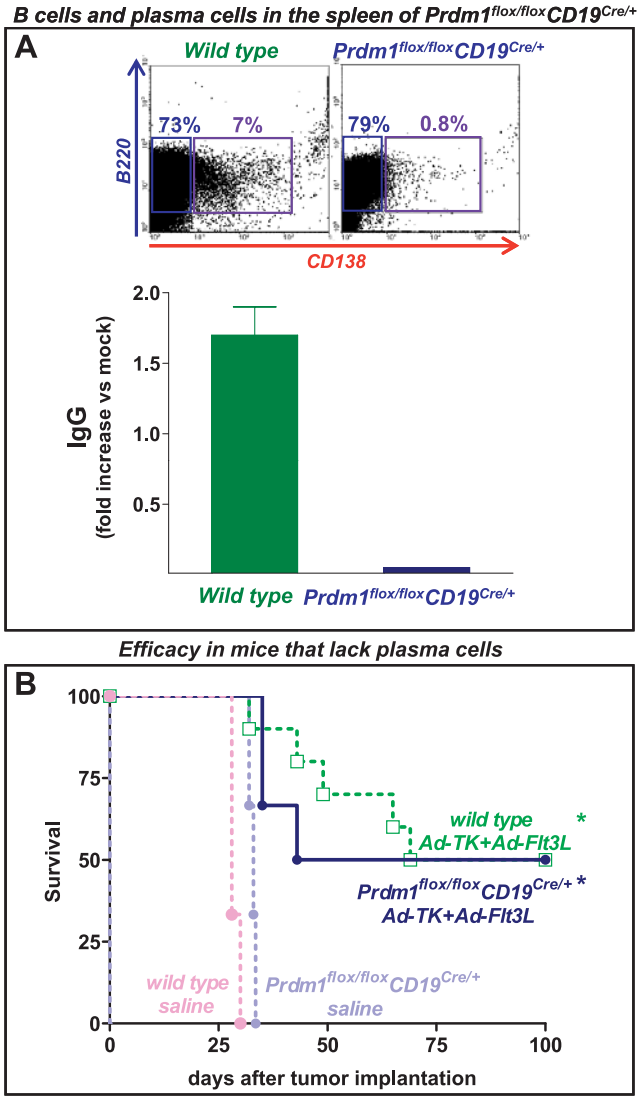

Figure 5. Lack of plasma cells does not impair the efficacy of Ad-TK+Ad-Flt3L. (A) Representative dot plots show the percentage of B cells ($B220^+$) and plasma cells ($B220^+CD138^+$) as assessed by flow cytometry. Note the lack of plasma cells in $Prdm1^{flox/flox}CD19^{Cre/+}$ mice. Splenocytes were collected from wild-type and $Prdm1^{flox/flox}CD19^{Cre/+}$ mice and incubated in the presence of 10 μg/ml LPS for 72 hours. Total IgG levels (IgG1, IgG2, IgG3, and IgG4) were assessed using an Easy-Titer IgG Assay Kit. (B) Kaplan-Meier curves show the survival of wild-type or $Prdm1^{flox/flox}CD19^{Cre/+}$ mice, which are unable to produce antibodies, that were implanted in the brain with GL26 cells and treated 14 days later with Ad-TK+Ad-Flt3L or saline. *$P < .05$ *versus* saline. Mantel log-rank test.

Using KO mice that are deficient in B cells ($Igh6^{-/-}$) and B cells' depleting antibodies, we found that B cells are required for the regression of intracranial GBM in mice treated with Ad-TK+Ad-Flt3L. Although administration of anti-CD20 antibody was reported to slow the growth of peripheral solid tumors and enhance the efficacy of immunotherapy [43], we found that administration of the anti-CD20 antibody did not affect the growth of untreated intracranial tumors in C57BL/6 mice and severely impaired the efficacy of Ad-TK+Ad-Flt3L gene therapy. Thus, although B-cell depletion may be a useful adjunct in immunotherapy for experimental B-cell lymphomas [44] and multiple nonhematopoietic solid tumor models, such as lung carcinoma, thymoma, and mesothelioma [43], our data suggest that B-cell depletion could be detrimental when inducing immune responses against tumors located within the central nervous system. Depletion of MZB cells also impaired the therapeutic effect of Ad-TK+Ad-Flt3L. MZB cells express high levels of MHCII and are potent activators of $CD4^+$ T cells [14]. Although in mice these cells are confined to the spleen, they have an ideal location to screen and rapidly respond to blood-borne antigens that may be released from dying tumor cells and to antigens that are transported by DCs [14]. MZB cells can transport IgM-containing immune complexes to follicular DCs in the initial steps of T-cell–dependent immune responses or can directly prime naive $CD4^+$ T cells, inducing their differentiation to effector T cells [16].

Although the antibody-mediated clearance of antigens located in the brain has been previously reported [45,46], our results indicate that the role of B cells in the antitumor immune response elicited in the intracranial tumor models does not seem to be through the production of tumor-opsonizing immunoglobulins: 1) we could not detect circulating antibodies in syngeneic GBM models using two different mouse strains, 2) we did not detect antibodies against tumor cells expressing a highly immunogenic surrogate tumor antigen, 3) the efficacy of Ad-TK+Ad-Flt3L was not impaired in mice that lack plasma cells, and 4) the efficacy of Ad-TK+Ad-Flt3L was impaired when mice received antibodies against CD20, which do not deplete plasma cells because of the loss of CD20 during plasma cell differentiation [32].

B cells can capture and present antigen [36,37] directly to T cells through MHC I [38,39] and II [9,40] after the up-regulation of coactivation markers on their cell surface [41]. The major route of antigen uptake by B cells is through specific binding to the B-cell receptor followed by receptor-mediated endocytosis. Antigen is then processed and loaded onto MHC molecules that are displayed on the B-cell surface. This process of antigen acquisition can be repeated as the B-cell encounters and binds additional antigen, thereby concentrating extracellular antigen encountered in low abundance, and subsequently present them to T cells [9]. B cells can present antigen [36,37] directly to T cells through MHC I [38,39] and II [9,40] after the up-regulation of coactivation markers on their cell surface [41]. Although cytotoxic $CD8^+$ T cells are involved in the immune-mediated rejection of the intracranial tumors [24], it has been demonstrated that tumor antigen–specific $CD8^+$ T cells are typically short-lived [47] and sustained T-cell–dependent immune responses require a concomitant $CD4^+$ T helper response to enhance the longevity of the $CD8^+$ T-cell response [48]. Herein, we assessed whether B cells purified from the LNs of OVA-GL26 tumor-bearing mice were capable of antigen presentation to $CD4^+$ T cells from OT-II transgenic mice. Only B cells from Ad-TK+Ad-Flt3L–treated mice were capable of providing costimulatory signals and tumor antigens supporting syngeneic T-cell proliferation. Our data suggest that B cells could be acting as APCs, playing a role in clonal expansion of tumor antigen–specific T lymphocytes.

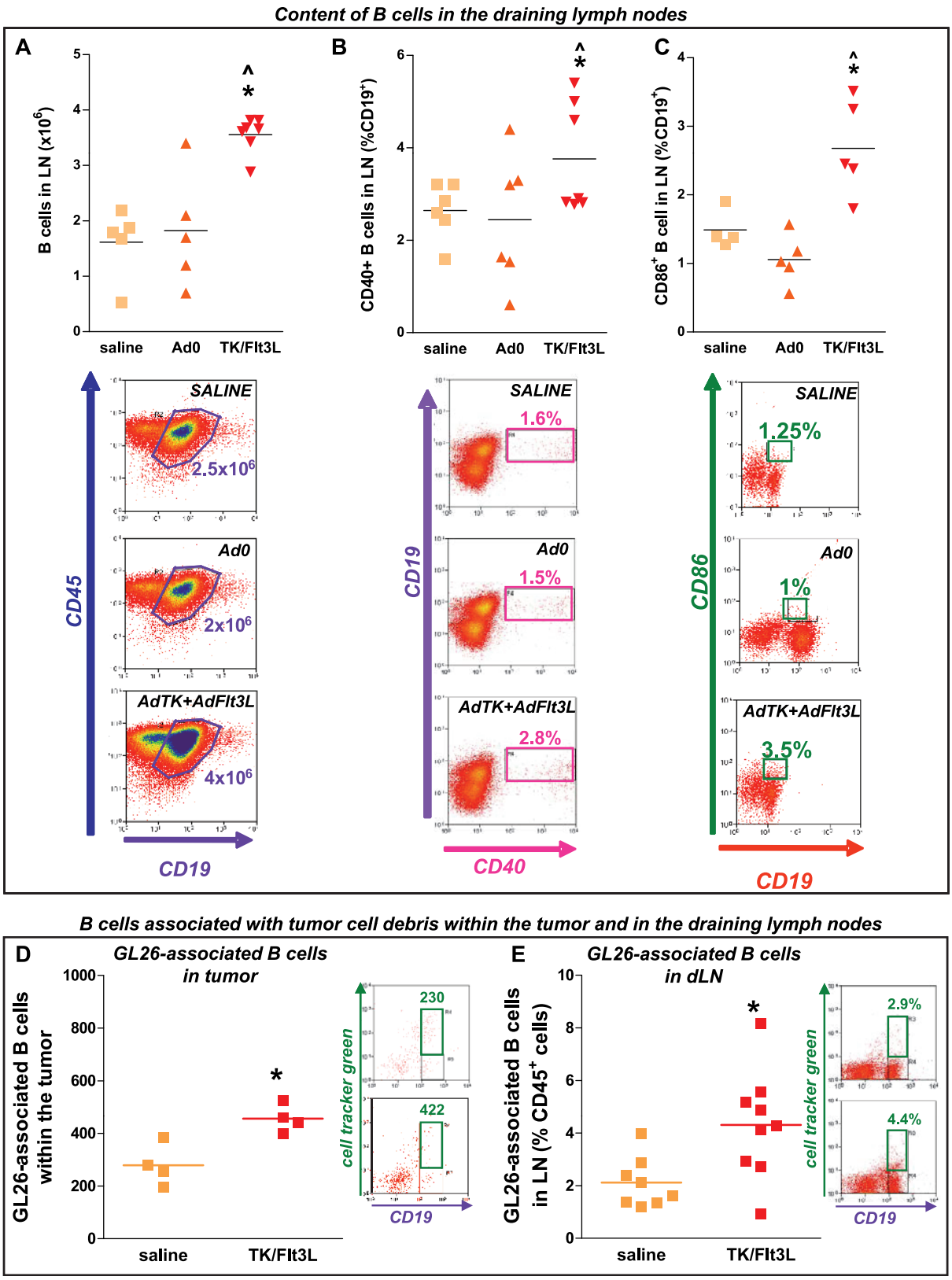

Figure 6. B cells containing tumor cell remnants migrate to the cervical draining LNs. Wild-type C57BL/6 mice were implanted with GL26 tumors and treated 14 days later with Ad-TK+Ad-Flt3L (Ad.TK/Flt3L), saline, or Ad.0. After 7 days, immune cells isolated from dLN were analyzed by flow cytometry. Representative dot plots and graphs show the content of B cells ($CD19^+/CD45^+$; A) and the percentage of $CD40^+$ ($CD19^+/CD45^+CD40^+$; B) and $CD86^+$ B cells ($CD19^+/CD45^+/CD86^+$; C) in the dLN. *$P < .05$ *versus* saline, ^$P < .05$ *versus* Ad.0 (one-way ANOVA followed by the Tukey test). (D and E) GL26 cells were labeled with CellTracker Green and implanted in the striatum of C57BL/6 mice. Two days later, mice were treated with either saline or Ad-TK+Ad-Flt3L and immune cells were isolated from tumors and draining LNs 7 days later. Representative dot plots and graphs show the content of B cells associated with CellTracker Green+ tumor protein remnants within the tumors (D) and in the dLN (E). *$P < .05$ (Student's *t* test).

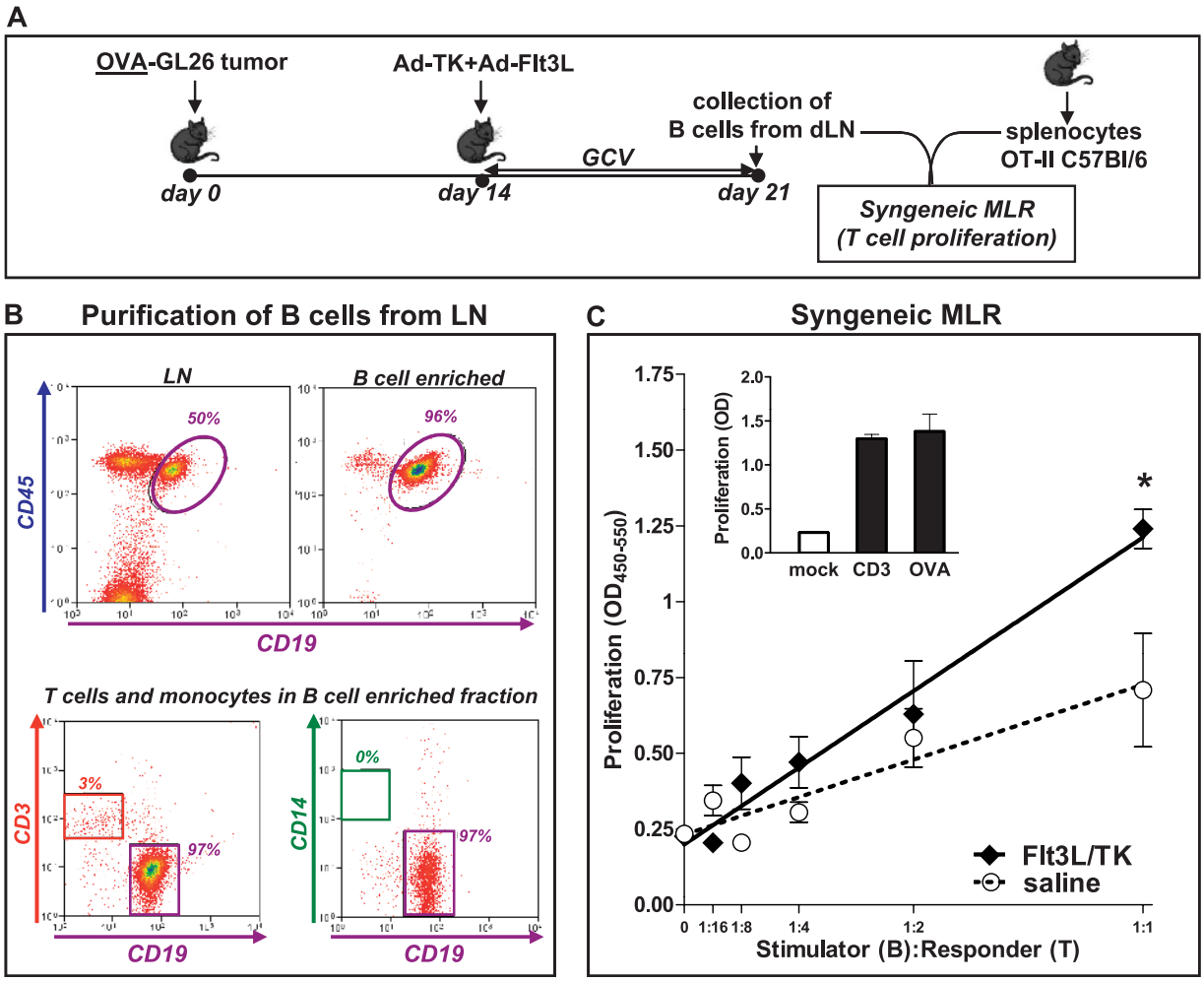

Figure 7. B cells isolated from the dLN of Ad-Flt3L– and Ad-TK–treated animals stimulate T-cell proliferation. (A) GL26 cells expressing the surrogate antigen chicken ovoalbumin (OVA) were implanted in the striatum of wild-type C57BL/6 mice and treated 14 days later with Ad-Flt3L and Ad-TK or saline. Seven days later, B cells were purified from the dLN by MACS. The purity of B-cell preparations was greater than 95%, as assessed by flow cytometry (B). (C) A syngeneic MLR was used to determine whether B cells could stimulate T-cell proliferation. B cells (stimulators) were primed with OVA, incubated with mitomycin, and then cocultured at different ratios with syngeneic splenocytes collected from naive OT-II mice (responders) for 72 hours. BrdU incorporation into DNA was used to determine cell proliferation. *$P < .05$ *versus* saline (randomization test). Inset: splenocytes were incubated in the absence of B cells and in the presence of anti-CD3 antibody (1 μg/ml) or $OVA_{323-339}$ (2 μg/ml), as positive controls.

In support of this, we found that B cells were required for the clonal expansion of tumor antigen–specific T cells. An alternative scenario is that B cells are not involved directly in presenting tumor antigen to T cells but could provide costimulatory signals to T cells in contact with DCs. This is supported by other studies that highlight the role of B cells to enhance the costimulatory signaling between DCs and T cells [49]. We have previously shown that DCs play a pivotal role in the onset of the antitumor immune response induced by Ad-TK+Ad-Flt3L [2]. Although DCs are the main APCs that trigger adaptive immune responses [50], increasing evidence suggests that interactions between DCs and B cells promote optimal T-cell activation. For instance, cooperation between DC and B cells has been observed to be required for the presentation of viral antigens to naive, antigen-specific T cells [51]. B cells have been shown to collaborate with DCs in the presentation of extracellular antigens that trigger the activation of effector T cells and the generation of memory T cells [49]. Furthermore, B cells have been shown to modulate the profile of cytokines released by activated DCs [52]. Conversely, DCs have been shown to capture, retain, and transfer unprocessed antigen to B cells [53]. Also, bidirectional proliferation and survival signaling have been detected between B cells and DCs [52,54].

Flt3L is a critical cytokine that induces differentiation of B cells from early hematopoietic stem cell precursors [34]. In our model, expression of Flt3L within the tumor mass resulted in high levels of systemic Flt3L, which may be responsible for the expansion of MZB cells and the increased levels of B cells observed in the dLN of tumor-bearing mice treated with Ad-TK+Ad-Flt3L. We also observed increased expression of cell surface CD40 and CD86 on B cells in the dLN, which is indicative that B cells are activated [55] and capable of acting as tumor APCs [41]. Our data suggests that B cells might be transporting tumor antigen and promoting T-cell proliferation in the draining LNs [36,56] after treatment with Ad-Flt3L/Ad-TK. Although the brain lacks classic lymph vessels, the migration of leukocytes from the brain to the cervical LNs has been shown to occur through the cribroid plate and the nasal mucosa [57]. Also, it is possible that

recirculating B cells encounter antigen in the LNs. Although the Ig receptor of B cells can bind soluble antigen, the efficiency of this process *in vivo* is very low. Nevertheless, it has been shown that, in the LNs, B cells can obtain antigens from subcapsular sinus macrophages and from follicular DCs, which can act as long-term depots for B-cell antigens [58]. These findings, and the fact that B cells from the LNs of Ad-Flt3L/Ad-TK–treated mice are able to stimulate the clonal expansion of syngeneic tumor antigen–specific T cells, strongly support the notion that B cells could be acting as APCs in this model. Although the number of B cells associated with tumor cell remnants that we detected in the cervical LNs (~400, i.e., ~60 per 10^6 cells) during the antitumor immune response induced by immunotherapy may seem small, it is in agreement with data from other groups. Lindell et al. [59] have shown that around 50 antigen-specific B cells/10^6 total cells reach the LNs to efficiently present cockroach antigen to T cells during the onset of allergic lung disease. It has also been demonstrated that only a few hundred skin-derived DCs are required to make their way to the draining brachial LN to provide prolonged presentation and robust levels of CTL expansion [60–62].

Taken together, the results we present in this article strongly suggest that B cells are acting as APCs. The evidence we present here can be summarized as follows: 1) B cells are required for antitumor immunity triggered by our treatment because the treatment fails in B-cell–deficient mice Igh6$^{-/-}$ mice and in wild-type mice that have been depleted of total B cells or MZB cells; 2) B cells' role in antitumor immunity does not depend on antibody production; 3) B cells have the ability to engulf tumor antigen, transport it to T-cell–rich areas, and overexpress coactivation markers that support T-cell activation; and 4) pure preparations of B cells from the LNs of Ad-Flt3L/Ad-TK–treated mice are able to stimulate the expansion of syngeneic tumor antigen–specific T cells.

The data presented herein indicate that B cells could be useful therapeutic targets to increase the efficacy of immunotherapeutics for brain cancer. It has been shown that CD40-activated B cells loaded with tumor RNA constitute potent antitumor vaccines, which can be readily generated from small amounts of blood and act as efficient APCs to drive the activation of antigen-specific T cells [22,63]. TLR9 agonists have also been shown to stimulate the expression of MHC and coactivation markers in human B cells, enhancing their ability to cross-present antigens to autologous T cells [64], and could improve B-cell vaccine design for brain cancer immune-based therapeutics. Our results highlight the role of B lymphocytes during immunotherapy-dependent brain tumor regression and suggest that they could act as APCs, leading to effective antitumor immunity and immunologic memory.

References

[1] Heimberger AB and Sampson JH (2011). Immunotherapy coming of age: what will it take to make it standard of care for glioblastoma? *Neuro Oncol* **13**, 3–13.

[2] Curtin J, Liu N, Candolfi M, Xiong W, Assi A, Yagiz K, Edwards M, Michelsen K, Kroeger K, Liu C, et al. (2009). HMGB1 mediates endogenous TLR2 activation and brain tumor regression. *PLoS Med* **6**, e10.

[3] Chien PY, Wang J, Carbonaro D, Lei S, Miller B, Sheikh S, Ali SM, Ahmad MU, and Ahmad I (2005). Novel cationic cardiolipin analogue-based liposome for efficient DNA and small interfering RNA delivery *in vitro* and *in vivo*. *Cancer Gene Ther* **12**, 321–328.

[4] Ghulam Muhammad AK, Candolfi M, King GD, Yagiz K, Foulad D, Mineharu Y, Kroeger KM, Treuer KA, Nichols WS, Sanderson NS, et al. (2009). Antiglioma immunological memory in response to conditional cytotoxic/immune–stimulatory gene therapy: humoral and cellular immunity lead to tumor regression. *Clin Cancer Res* **15**, 6113–6127.

[5] Dong HP, Elstrand MB, Holth A, Silins I, Berner A, Trope CG, Davidson B, and Risberg B (2006). NK- and B-cell infiltration correlates with worse outcome in metastatic ovarian carcinoma. *Am J Clin Pathol* **125**, 451–458.

[6] Nzula S, Going JJ, and Stott DI (2003). Antigen-driven clonal proliferation, somatic hypermutation, and selection of B lymphocytes infiltrating human ductal breast carcinomas. *Cancer Res* **63**, 3275–3280.

[7] Kotlan B, Simsa P, Teillaud JL, Fridman WH, Toth J, McKnight M, and Glassy MC (2005). Novel ganglioside antigen identified by B cells in human medullary breast carcinomas: the proof of principle concerning the tumor-infiltrating B lymphocytes. *J Immunol* **175**, 2278–2285.

[8] de Visser KE, Korets LV, and Coussens LM (2005). *De novo* carcinogenesis promoted by chronic inflammation is B lymphocyte dependent. *Cancer Cell* **7**, 411–423.

[9] Rodriguez-Pinto D (2005). B cells as antigen presenting cells. *Cell Immunol* **238**, 67–75.

[10] Inoue S, Leitner WW, Golding B, and Scott D (2006). Inhibitory effects of B cells on antitumor immunity. *Cancer Res* **66**, 7741–7747.

[11] Shah S, Divekar AA, Hilchey SP, Cho HM, Newman CL, Shin SU, Nechustan H, Challita-Eid PM, Segal BM, Yi KH, et al. (2005). Increased rejection of primary tumors in mice lacking B cells: inhibition of anti-tumor CTL and T_H1 cytokine responses by B cells. *Int J Cancer* **117**, 574–586.

[12] Perricone MA, Smith KA, Claussen KA, Plog MS, Hempel DM, Roberts BL, St George JA, and Kaplan JM (2004). Enhanced efficacy of melanoma vaccines in the absence of B lymphocytes. *J Immunother* **27**, 273–281.

[13] Li Q, Grover AC, Donald EJ, Carr A, Yu J, Whitfield J, Nelson M, Takeshita N, and Chang AE (2005). Simultaneous targeting of CD3 on T cells and CD40 on B or dendritic cells augments the antitumor reactivity of tumor-primed lymph node cells. *J Immunol* **175**, 1424–1432.

[14] Pillai S, Cariappa A, and Moran ST (2005). Marginal zone B cells. *Annu Rev Immunol* **23**, 161–196.

[15] Cinamon G, Zachariah MA, Lam OM, Foss FW Jr, and Cyster JG (2008). Follicular shuttling of marginal zone B cells facilitates antigen transport. *Nat Immunol* **9**, 54–62.

[16] Lopes-Carvalho T, Foote J, and Kearney JF (2005). Marginal zone B cells in lymphocyte activation and regulation. *Curr Opin Immunol* **17**, 244–250.

[17] Serreze DV, Fleming SA, Chapman HD, Richard SD, Leiter EH, and Tisch RM (1998). B lymphocytes are critical antigen-presenting cells for the initiation of T cell–mediated autoimmune diabetes in nonobese diabetic mice. *J Immunol* **161**, 3912–3918.

[18] Chan OT, Hannum LG, Haberman AM, Madaio MP, and Shlomchik MJ (1999). A novel mouse with B cells but lacking serum antibody reveals an antibody-independent role for B cells in murine lupus. *J Exp Med* **189**, 1639–1648.

[19] Takemura S, Klimiuk PA, Braun A, Goronzy JJ, and Weyand CM (2001). T cell activation in rheumatoid synovium is B cell dependent. *J Immunol* **167**, 4710–4718.

[20] Lapointe R, Bellemare-Pelletier A, Housseau F, Thibodeau J, and Hwu P (2003). CD40-stimulated B lymphocytes pulsed with tumor antigens are effective antigen-presenting cells that can generate specific T cells. *Cancer Res* **63**, 2836–2843.

[21] von Bergwelt-Baildon M, Schultze JL, Maecker B, Menezes I, and Nadler LM (2004). Correspondence re R. Lapointe et al., CD40-stimulated B lymphocytes pulsed with tumor antigens are effective antigen-presenting cells that can generate specific T cells. *Cancer Res* 2003;63:2836–43. *Cancer Res* **64**, 4055–4056; author reply 4056–4057.

[22] Schultze JL, Michalak S, Seamon MJ, Dranoff G, Jung K, Daley J, Delgado JC, Gribben JG, and Nadler LM (1997). CD40-activated human B cells: an alternative source of highly efficient antigen presenting cells to generate autologous antigen-specific T cells for adoptive immunotherapy. *J Clin Invest* **100**, 2757–2765.

[23] Shapiro-Shelef M, Lin KI, McHeyzer-Williams LJ, Liao J, McHeyzer-Williams MG, and Calame K (2003). Blimp-1 is required for the formation of immunoglobulin secreting plasma cells and pre-plasma memory B cells. *Immunity* **19**, 607–620.

[24] Yang J, Sanderson NSR, Wawrowsky K, Puntel M, Castro MG, and Lowenstein PR (2010). Kupfer-type immunological synapse characteristics do not predict anti-brain tumor cytolytic T-cell function *in vivo*. *Proc Natl Acad Sci USA* **107**, 4716–4721.

[25] Sampson JH, Ashley DM, Archer GE, Fuchs HE, Dranoff G, Hale LP, and Bigner DD (1997). Characterization of a spontaneous murine astrocytoma and abrogation of its tumorigenicity by cytokine secretion. *Neurosurgery* **41**, 1365–1372; discussion 1372–1363.

[26] Yu S, Dunn R, Kehry MR, and Braley-Mullen H (2008). B cell depletion inhibits spontaneous autoimmune thyroiditis in NOD.H-2h4 mice. *J Immunol* **180**, 7706–7713.
[27] Lu TT and Cyster JG (2002). Integrin-mediated long-term B cell retention in the splenic marginal zone. *Science* **297**, 409–412.
[28] Candolfi M, Yagiz K, Foulad D, Alzadeh GE, Tesarfreund M, Muhammad AK, Puntel M, Kroeger KM, Liu C, Lee S, et al. (2009). Release of HMGB1 in response to proapoptotic glioma killing strategies: efficacy and neurotoxicity. *Clin Cancer Res* **15**, 4401–4414.
[29] Robertson JM, Jensen PE, and Evavold BD (2000). DO11.10 and OT-II T cells recognize a C-terminal ovalbumin 323-339 epitope. *J Immunol* **164**, 4706–4712.
[30] Hussain SF, Yang D, Suki D, Aldape K, Grimm E, and Heimberger AB (2006). The role of human glioma-infiltrating microglia/macrophages in mediating antitumor immune responses. *Neuro Oncol* **8**, 261–279.
[31] Ngo VN, Cornall RJ, and Cyster JG (2001). Splenic T zone development is B cell dependent. *J Exp Med* **194**, 1649–1660.
[32] DiLillo DJ, Hamaguchi Y, Ueda Y, Yang K, Uchida J, Haas KM, Kelsoe G, and Tedder TF (2008). Maintenance of long-lived plasma cells and serological memory despite mature and memory B cell depletion during CD20 immunotherapy in mice. *J Immunol* **180**, 361–371.
[33] Belperron AA, Dailey CM, Booth CJ, and Bockenstedt LK (2007). Marginal zone B-cell depletion impairs murine host defense against *Borrelia burgdorferi* infection. *Infect Immun* **75**, 3354–3360.
[34] Ray RJ, Paige CJ, Furlonger C, Lyman SD, and Rottapel R (1996). Flt3 ligand supports the differentiation of early B cell progenitors in the presence of interleukin-11 and interleukin-7. *Eur J Immunol* **26**, 1504–1510.
[35] Buza-Vidas N, Cheng M, Duarte S, Nozad H, Jacobsen SE, and Sitnicka E (2007). Crucial role of FLT3 ligand in immune reconstitution after bone marrow transplantation and high-dose chemotherapy. *Blood* **110**, 424–432.
[36] Carrasco YR and Batista FD (2007). B cells acquire particulate antigen in a macrophage-rich area at the boundary between the follicle and the subcapsular sinus of the lymph node. *Immunity* **27**, 160–171.
[37] Okada T, Miller MJ, Parker I, Krummel MF, Neighbors M, Hartley SB, O'Garra A, Cahalan MD, and Cyster JG (2005). Antigen-engaged B cells undergo chemotaxis toward the T zone and form motile conjugates with helper T cells. *PLoS Biol* **3**, e150.
[38] Hon H, Oran A, Brocker T, and Jacob J (2005). B lymphocytes participate in cross-presentation of antigen following gene gun vaccination. *J Immunol* **174**, 5233–5242.
[39] Hoft DF, Eickhoff CS, Giddings OK, Vasconcelos JR, and Rodrigues MM (2007). Trans-sialidase recombinant protein mixed with CpG motif-containing oligodeoxynucleotide induces protective mucosal and systemic *Trypanosoma cruzi* immunity involving $CD8^+$ CTL and B cell–mediated cross-priming. *J Immunol* **179**, 6889–6900.
[40] Clark MR, Massenburg D, Siemasko K, Hou P, and Zhang M (2004). B-cell antigen receptor signaling requirements for targeting antigen to the MHC class II presentation pathway. *Curr Opin Immunol* **16**, 382–387.
[41] Evans DE, Munks MW, Purkerson JM, and Parker DC (2000). Resting B lymphocytes as APC for naive T lymphocytes: dependence on CD40 ligand/CD40. *J Immunol* **164**, 688–697.
[42] Croft M (1994). Activation of naive, memory and effector T cells. *Curr Opin Immunol* **6**, 431–437.
[43] Kim S, Fridlender ZG, Dunn R, Kehry MR, Kapoor V, Blouin A, Kaiser LR, and Albelda SM (2008). B-cell depletion using an anti-CD20 antibody augments antitumor immune responses and immunotherapy in nonhematopoetic murine tumor models. *J Immunother* **31**, 446–457.
[44] Gadri Z, Kukulansky T, Bar-Or E, Haimovich J, and Hollander N (2009). Synergistic effect of dendritic cell vaccination and anti-CD20 antibody treatment in the therapy of murine lymphoma. *J Immunother* **32**, 333–340.
[45] Vasilevko V, Xu F, Previti ML, Van Nostrand WE, and Cribbs DH (2007). Experimental investigation of antibody-mediated clearance mechanisms of amyloid-β in CNS of Tg-SwDI transgenic mice. *J Neurosci* **27**, 13376–13383.
[46] Ankeny DP and Popovich PG (2011). B cells and autoantibodies: complex roles in CNS injury. *Trends Immunol* **31**, 332–338.
[47] Dudley ME, Wunderlich J, Nishimura MI, Yu D, Yang JC, Topalian SL, Schwartzentruber DJ, Hwu P, Marincola FM, Sherry R, et al. (2001). Adoptive transfer of cloned melanoma-reactive T lymphocytes for the treatment of patients with metastatic melanoma. *J Immunother* **24**, 363–373.
[48] Knutson KL, Schiffman K, Cheever MA, and Disis ML (2002). Immunization of cancer patients with a HER-2/*neu*, HLA-A2 peptide, p369-377, results in short-lived peptide-specific immunity. *Clin Cancer Res* **8**, 1014–1018.
[49] Crawford A, Macleod M, Schumacher T, Corlett L, and Gray D (2006). Primary T cell expansion and differentiation *in vivo* requires antigen presentation by B cells. *J Immunol* **176**, 3498–3506.
[50] Brigl M and Brenner MB (2004). CD1: antigen presentation and T cell function. *Annu Rev Immunol* **22**, 817–890.
[51] Diaz-de-Durana Y, Mantchev GT, Bram RJ, and Franco A (2006). TACI-BLyS signaling via B-cell–dendritic cell cooperation is required for naive $CD8^+$ T-cell priming *in vivo*. *Blood* **107**, 594–601.
[52] Moulin V, Andris F, Thielemans K, Maliszewski C, Urbain J, and Moser M (2000). B lymphocytes regulate dendritic cell (DC) function *in vivo*: increased interleukin 12 production by DCs from B cell-deficient mice results in T helper cell type 1 deviation. *J Exp Med* **192**, 475–482.
[53] Wykes M, Pombo A, Jenkins C, and MacPherson GG (1998). Dendritic cells interact directly with naive B lymphocytes to transfer antigen and initiate class switching in a primary T-dependent response. *J Immunol* **161**, 1313–1319.
[54] Wykes M and MacPherson G (2000). Dendritic cell–B-cell interaction: dendritic cells provide B cells with CD40-independent proliferation signals and CD40-dependent survival signals. *Immunology* **100**, 1–3.
[55] Constant S, Schweitzer N, West J, Ranney P, and Bottomly K (1995). B lymphocytes can be competent antigen-presenting cells for priming $CD4^+$ T cells to protein antigens *in vivo*. *J Immunol* **155**, 3734–3741.
[56] Attanavanich K and Kearney JF (2004). Marginal zone, but not follicular B cells, are potent activators of naive CD4 T cells. *J Immunol* **172**, 803–811.
[57] Goldmann J, Kwidzinski E, Brandt C, Mahlo J, Richter D, and Bechmann I (2006). T cells traffic from brain to cervical lymph nodes via the cribroid plate and the nasal mucosa. *J Leukoc Biol* **80**, 797–801.
[58] Gonzalez SF, Degn SE, Pitcher LA, Woodruff M, Heesters BA, and Carroll MC (2011). Trafficking of B cell antigen in lymph nodes. *Annu Rev Immunol* **29**, 215–233.
[59] Lindell DM, Berlin AA, Schaller MA, and Lukacs NW (2008). B cell antigen presentation promotes T_H2 responses and immunopathology during chronic allergic lung disease. *PLoS One* **3**, e3129.
[60] Stock AT, Mueller SN, van Lint AL, Heath WR, and Carbone FR (2004). Cutting edge: prolonged antigen presentation after herpes simplex virus-1 skin infection. *J Immunol* **173**, 2241–2244.
[61] Allan RS, Waithman J, Bedoui S, Jones CM, Villadangos JA, Zhan Y, Lew AM, Shortman K, Heath WR, and Carbone FR (2006). Migratory dendritic cells transfer antigen to a lymph node–resident dendritic cell population for efficient CTL priming. *Immunity* **25**, 153–162.
[62] Cumberbatch M and Kimber I (1995). Tumour necrosis factor-α is required for accumulation of dendritic cells in draining lymph nodes and for optimal contact sensitization. *Immunology* **84**, 31–35.
[63] Coughlin CM, Vance BA, Grupp SA, and Vonderheide RH (2004). RNA-transfected CD40-activated B cells induce functional T-cell responses against viral and tumor antigen targets: implications for pediatric immunotherapy. *Blood* **103**, 2046–2054.
[64] Jiang W, Lederman MM, Harding CV, and Sieg SF (2011). Presentation of soluble antigens to $CD8^+$ T cells by CpG oligodeoxynucleotide-primed human naive B cells. *J Immunol* **186**, 2080–2086.

Table W1. Source of Antibodies.

Antibody	Catalog No.
Depletion	
Anti–LFA-1 (αLβ2)	553118 (BD Pharmingen)
Anti–CD49d (α4)	553154 (BD Pharmingen)
Rat IgG2a	553927 (BD Pharmingen)
Rat IgG2b	553986 (BD Pharmingen)
Flow cytometry	
Anti-CD45	560501 (BD Pharmingen)
Anti-CD19	561113 (BD Pharmingen)
Anti-CD138	553714 (BD Pharmingen)
Anti-CD40	558695 (BD Pharmingen)
Anti-CD86	553768 (BD Pharmingen)
Anti-CD21	552957 (BD Pharmingen)
Anti-B220	553138 (BD Pharmingen)
Anti-CD3	553063 (BD Pharmingen)
Anti-CD8 alpha	553035 (BD Pharmingen)
Anti-CD4	553052 (BD Pharmingen)
Anti-CD14	553063 (BD Pharmingen)
Immunocytochemistry	
Anti-CD19	MCA1439GA (Serotec, Oxford, United Kingdom)
Anti-vimentin	NB100-92123 (Novus Biological, Littleton, CO)
$Alexa_{594}$-conjugated goat anti-rat IgG	A-11007 (Invitrogen)
$Alexa_{488}$-conjugated goat anti-rabbit IgG	A-11034 (Invitrogen)

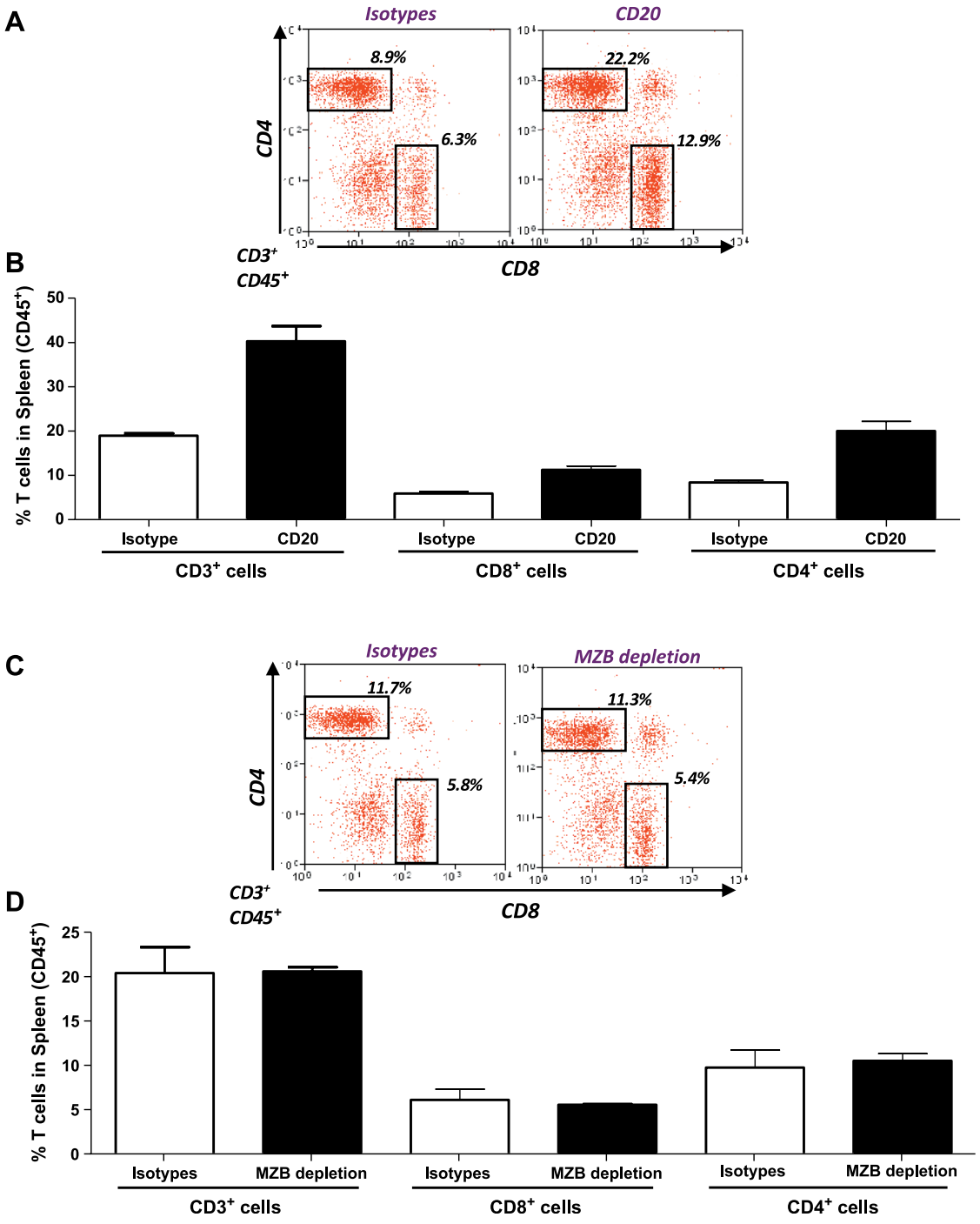

Figure W1. Administration of antimouse CD20 antibodies or MZB depleting antibodies does not deplete T cells. (A) Representative dot plots show the populations of T lymphocytes in the spleen of naive mice injected i.p. with mouse antimouse CD20 antibody (IgG2a, 300 μg) or with isotype control (mouse anti-human CD20 IgG2a, 300 μg). (B) Spleens were collected 7 days after depletion and total $CD3^+$ lymphocytes, $CD4^+$ T cells, and $CD8^+$ T cells ($CD45^+/CD3^+$ and $CD4^+$ or $CD8^+$, respectively) were quantified by flow cytometry. (C) Representative dot plots show the populations of T lymphocytes in the spleen of naive mice injected i.p. with anti-CD49d antibody (100 μg) and anti–LFA-1 antibody (100 μg) or the corresponding isotype controls (rat IgG2a and rat IgG2b, 100 μg each). (D) Spleens were collected 7 days after depletion, and total $CD3^+$ lymphocytes and CD4 and CD8 T cells ($CD45^+/CD3^+$ and $CD4^+$ or $CD8^+$), respectively, were quantified by flow cytometry.

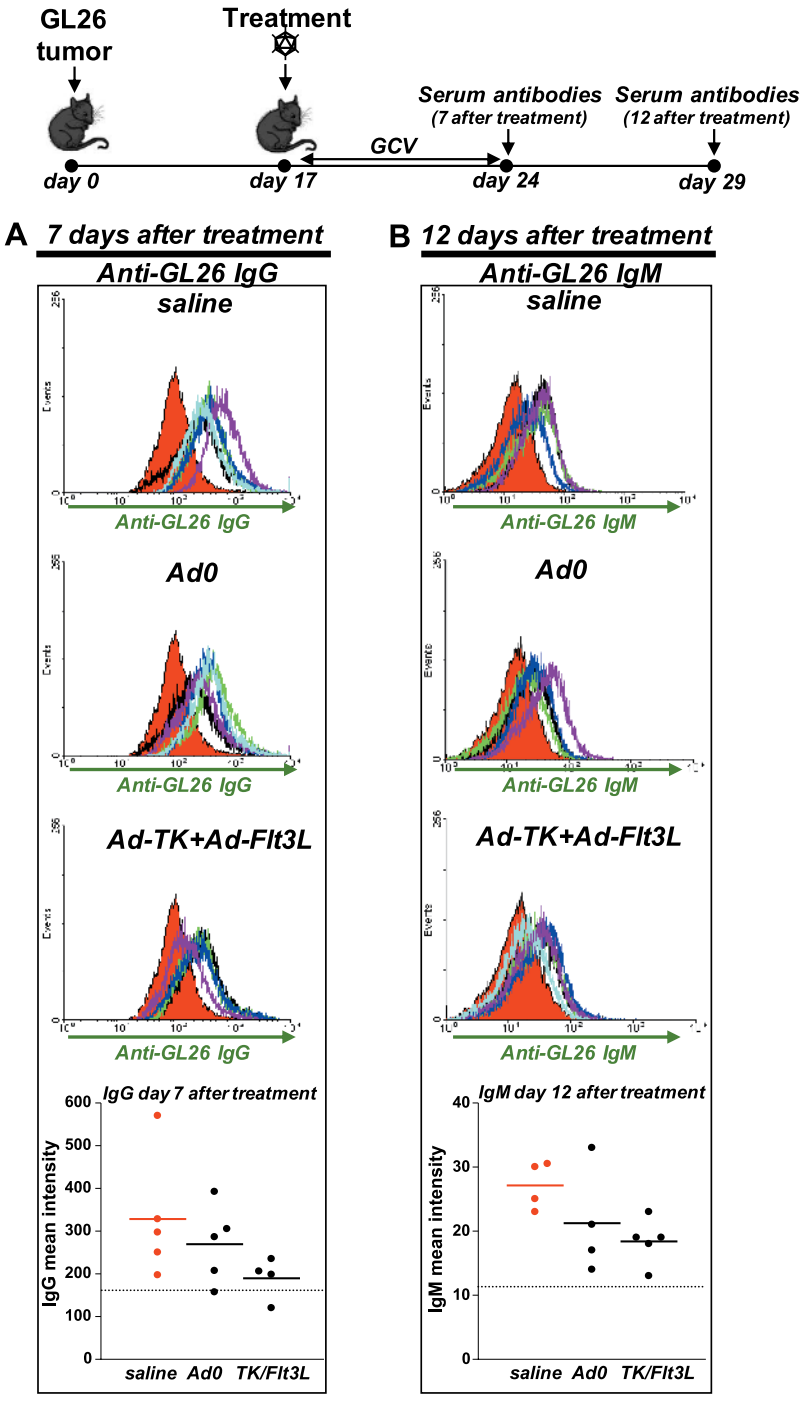

Figure W2. Assessment of the antibody response against the tumor. GL26 cells were implanted in the striatum of C57BL/6 mice and treated 14 days later with an intratumoral injection of Ad-TK+Ad-Flt3L, saline, or an empty vector (Ad.0). At 7 (A) and 12 (B) days after the treatment, serum was collected to evaluate the presence of circulating anti-GL26 cell IgG (A) and IgM (B), respectively. Histograms and graphs show the fluorescence intensity of fixed GL26 cells that were incubated with normal C57BL/6 serum (red area) or serum from treated tumor-bearing mice (colored lines), followed by FITC-conjugated antimouse IgM or IgG.

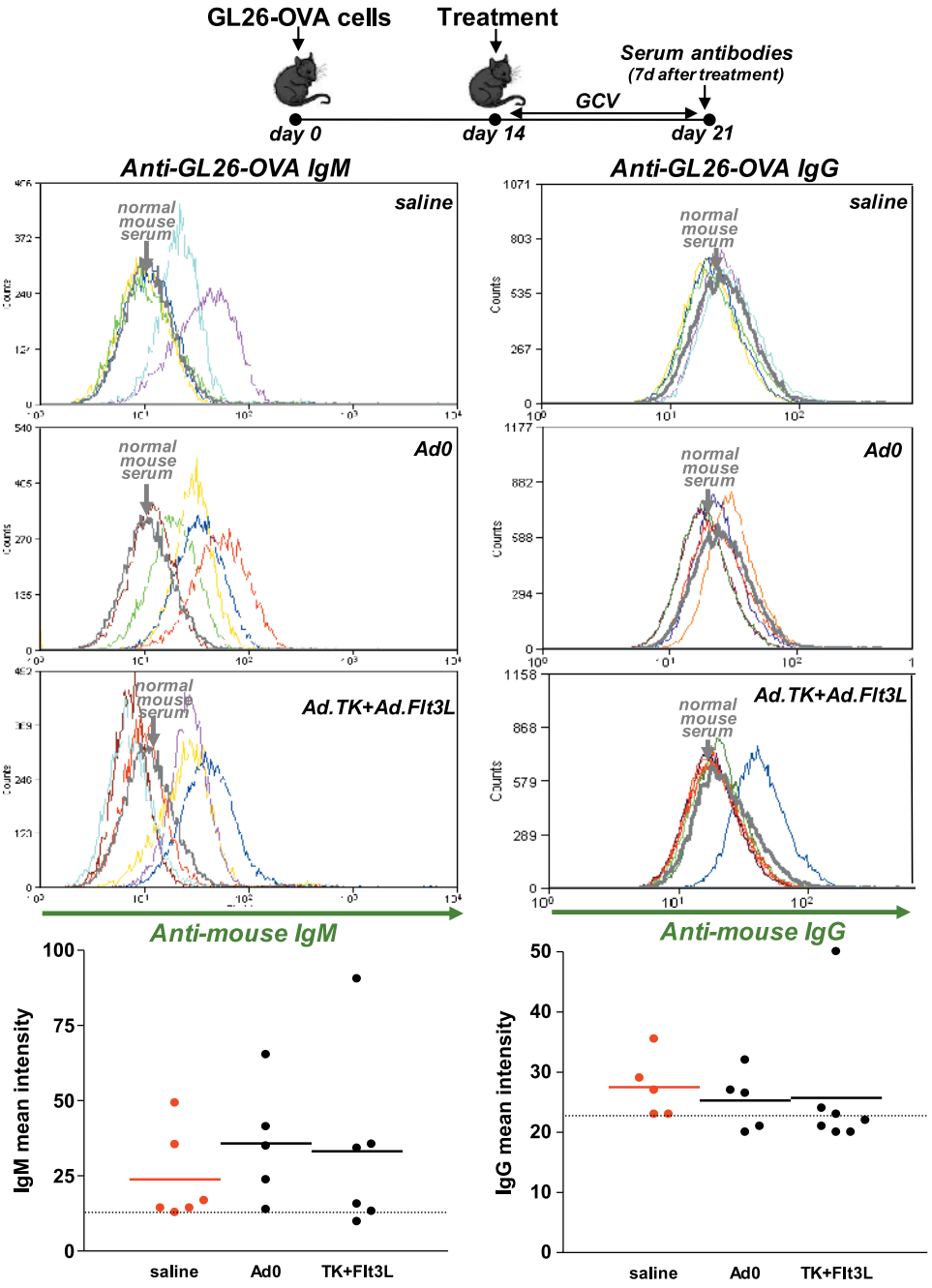

Figure W3. Assessment of the antibody response against tumor cells expressing a surrogate antigen. GL26 cells expressing chicken ovalbumin (GL26-OVA) were implanted in the striatum of C57BL/6 mice and treated 14 days later with an intratumoral injection of Ad-TK+Ad-Flt3L, saline, or an empty vector (Ad.0). Seven days after the treatment, serum was collected to evaluate the presence of circulating anti–GL26-OVA cell IgM and IgG. Histograms and graphs show the fluorescence intensity of fixed GL26-OVA cells that were incubated with normal C57BL/6 serum (red area) or serum from treated tumor-bearing mice (colored lines), followed by FITC-conjugated antimouse IgM or IgG.

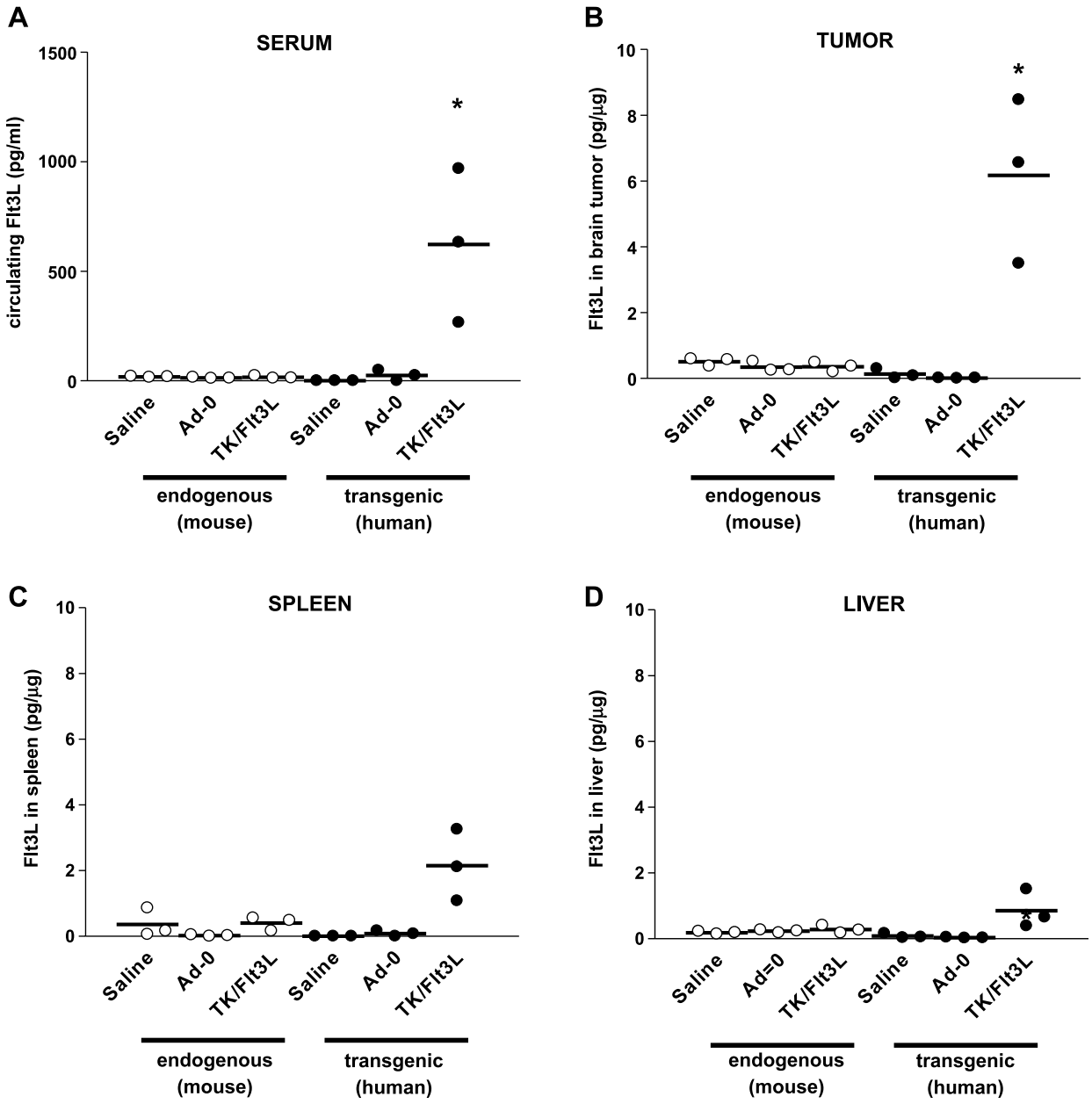

Figure W4. Flt3L expression 7 days after intratumoral delivery of Ad-Flt3L and Ad-TK. (A) GL26 tumor cells were implanted into the striatum of C57BL/6 mice; tumors were treated 14 days later with saline (S), Ad.0, or Ad-TK+Ad-Flt3L (TF). Levels of Flt3L expressed from the Ad vector were assessed using an ELISA specific for human Flt3L (transgenic). Levels of endogenous Flt3L were assessed using an ELISA specific for mouse Flt3L. Serum (A), brain tumors (B), spleen (C), and liver (D) were harvested 7 days after treatment, and both endogenous and transgenic Flt3L levels were assayed by ELISA. *$P < .05$ *versus* corresponding saline. Two-way ANOVA followed by the Tukey test.